IMPACT OF TORREFACTION ON GRINDABILITY, HYDROPHOBICITY AND FUEL CHARACTERISTICS OF BIOMASS RELEVANT TO HAWAIʻI

A THESIS SUBMITTED TO THE GRADUATE DIVISION OF THE UNIVERSITY OF HAWAIʻI AT MĀNOA IN PARTIAL FULFILLMENT OF THE REQUIREMENTS FOR THE DEGREE OF

MASTER OF SCIENCE

IN

MECHANICAL ENGINEERING

DECEMBER 2015

By

Dong Li

Thesis Committee:

Scott Turn, Chairperson

Stephen Masutani

Andrew Hashimoto

Keywords: Torrefaction, Biomass, Pretreatment, Fuel

- **Abstract**

Torrefaction is a thermal treatment process that can significantly improve fuel properties of solid biomass, provide alternative fuel source for coal fired plants, and contribute to greenhouse gas emission mitigation.

This thesis studied the impact of torrefaction on selected tropical biomass: leucaena, energy cane, eucalyptus, sugarcane, sugar cane bagasse and purple banagrass, at torrefaction temperatures of 182, 206, 220, 248 and 273°C. Dewatering/leaching treatment was used on energy cane, sugarcane and purple banagrass. Fuel properties, including heating value, mass, energy yield and ultimate, proximate analysis, were determined. All biomass species generally experienced an increase in mass loss and HHV with rising temperature. Energy yield for woody and dewatered/leached (S3) grass biomass was substantially larger than parent grass species (S0) that were not subjected to dewatering/leaching. Proximate analysis verified that increasing torrefaction temperature resulted in increased fixed carbon content and decreased volatile matter content. A Van Krevelen diagram constructed from ultimate analysis data was presented.

The research also explored about the grindability and hydrophobicity characteristics of all samples. Torrefaction improved the grindability and temperatures of 200 to 225 °C are recommended to attain comparable grinding behavior to coal commonly used in Hawaii. Leucaena was the exception, requiring a torrefaction temperature of 260 °C to achieve similar results.

Torrefaction generally improved the hydrophobicity characteristics of all samples and hydrophobicity increased with increasing torrefaction temperature. Woody and dewatered/leached grass species were more hydrophobic than grass species that were not dewatered/leached.

- **Table of contents**

- **List of tables**

- **List of figures**

- **1. Introduction**

In this chapter an introduction to the world energy situation, renewable energy development and biomass torrefaction is presented and the objectives of this thesis are identified.

World population has increased explosively from 1.65 billion in 1900 to over 7 billion in 2015. In order to meet the energy demand of a growing and increasingly prosperous world population, the world's primary energy demand almost doubled over the past 35 years. According to the IEA World Energy Outlook, energy demand increased from about 7.2 billion TOE (tons of oil equivalent) in 1980 to a projected 14.1 billion TOE in 2015. 80% of the world's primary energy was generated by fossil fuels in 2011 [1]. However, there are many concerns about the dominant position of fossil fuels. Carbon dioxide emissions are increasing at an alarming rate leading to global warming and climate change. Particulate matter, CO, unburned hydrocarbons, SO_2, and NO_x produced by fossil fuel conversion cause local and regional pollution. Our dependence on fossil fuels also brings about economic and security risks.

Population explosion, increasing energy consumption, rising fossil fuel prices, and policies designed to counter global warming have focused increasing attention on renewable energy. During the last decade, renewable energy has grown at a much faster rate than fossil fuel use and has become an important component of energy supply. In 2011, renewable energy provided 9.75 EJ, compared to 25.84 EJ of petroleum and 23.40 EJ of coal. Renewable energy technologies in the power sector will be applied in more than 70 countries worldwide by 2017 [2].Policies in support of renewable energy aim at reducing emissions of carbon dioxide and pollutants and also diversifying energy supplies to enhance energy security. Fossil fuel prices are expected to

increase for the foreseeable future which will make renewables more attractive to many investors.

Biomass is generally defined as biological material derived from plants or animals as well as their waste and residues [3]. Biomass is a significant contributor to renewable energy resources and has great potential for expansion in the future.

In 2011, biomass provided 4.65 EJ as a primary energy source whereas renewable energy production from hydroelectric power, geothermal, solar thermal/photovoltaic, wind, and biomass amounts to 9.64 EJ [1]. According to the 2012 Annual Energy Outlook published by the U.S. Department of Energy (DoE) and Energy Information Administration (EIA), production of biomass energy will have the highest annual growth (3.3%) from 2010 to 2035, compared to other energy supplies, e.g. crude oil, dry natural gas, coal, and nuclear [2].

Biomass can be converted to dispatchable heat and power in line with demand. This is an advantage over photovoltaic and wind power making biomass an important pillar in the energy supply. Furthermore, wide use of biomass can create new industries and new jobs, thereby boosting the economies of agricultural regions with an abundance of energy crops. As an archipelago in the central Pacific Ocean, Hawaii produces about 88% of its electricity and 96% of its liquid fuels from fossil fuels [4]. Hawaii has adopted ambitious goals for the development of renewable energy. A prominent example is the Hawaiian Electric Company's (HECO) stated goal in their Clean Energy Update [5] of 2012: "In 2011, 12% of electricity sales came from renewable sources, well on our way to Hawaii's next renewable mandate: 15% by 2015. More than 1,000 MW of renewable projects are in service, under construction, awaiting approval or being negotiated with more to come." Among all kinds of renewable energy, biomass is currently the only potential source of renewable transportation fuel to meet the State of Hawaii alternate

fuel target of 20% of motor gasoline consumption. Biomass resources could be a significant contributor to Hawaii's renewable energy future [6].According to the Hawaii Clean Energy Leader list (updated July 2015), biofuel and biomass projects rank among the top planned energy developments and are progressing toward becoming commercial enterprises.

Untreated biomass can have significant drawbacks as fuel that include relatively high moisture content, inhomogeneous physical structure and properties, non-uniform particle size, low energy density and biodegradability. These cause problems during transport, handling, conversion and storage and can also limit the number of suitable applications. For example, owing to its fibrous structure, biomass is less brittle than coal and this characteristic is particularly relevant when co-firing biomass in pulverized coal combustion systems [7,8], as different grinding equipment may be required for the two fuels.

In order to address these challenges and generally enhance biomass properties, the pre-treatment process of torrefaction has been proposed. Objectives of this thesis include evaluating torrefaction of tropical biomass materials over a range of treatment temperatures, analyzing the fuel properties of torrefied products and developing analytical methods to measure improvements in grindability and hydrophobicity.

The following chapter will review the process of torrefaction.

- **2. Literature review**

This chapter reviews recent progress in torrefaction processes, diversity of samples treated, and biomass material property changes from torrefaction.

2.1 Torrefaction

This section describes torrefaction processes and technology.

2.1.1 General description

The torrefaction process, also described as roasting, mild pyrolysis, or high temperature drying, is designed to improve the properties of biomass with the goal of having them approach those of coal.

Torrefaction is a thermal treatment process for biomass operating in a temperature range of 200 – 300°C. Generally, it is accomplished with an inert atmosphere, a low heating rate (10 – 30°C min^{-1}), and a residence time of 15 – 60 min [9,10,13–18]. During torrefaction, volatiles or torrefied gases are liberated and the remaining solid is the final product called torrefied biomass or torrefied fuel. When the inert gas is replaced by a high pressure liquid (about 45 bar), the process is called wet torrefaction or hydrothermal pretreatment [14–17].

Indicators of torrefaction performance include mass yield and energy yield. Mass yield (η_m) is defined as:

$$\eta_m = \frac{m_t}{m_o} \quad (1)$$

where m_o is the dry mass of the feedstock and m_t is the dry mass of the torrefied product. Similarly, energy yield (η_e) is defined as:

$$\eta_e = \eta_m \frac{HHV_t}{HHV_o} \quad (2)$$

where HHV_o is the higher heating value of the dry feedstock and HHV_t is the higher heating value of the dry torrefied product.

Uemura et al. [9] studied the effect of oxygen on torrefaction of oil palm wastes and found that the torrefaction reaction rate was affected only by the temperature. Oxygen concentration and biomass particle size had no significant effects on the reaction rate. An increase in oxygen concentration from 3 to 15% at 300°C resulted in slight decreases in mass and energy yields (90.3to 89.5% and 107.3 to 106.3%), respectively. It is interesting to note that the energy yield is greater than 100% and was not explained by the authors.

The concept of torrefaction was first elaborated in the 1930's when research was conducted in France on torrefied woody biomass for gasifier applications [18].After that, the use of torrefied wood to replace charcoal in metallurgy was pioneered. The Pechiney company built a torrefaction demonstration plant that was capable of producing 12,000 tons of torrefied materials per year [19] until it was dismantled in the 1990's. During the last ten years, torrefaction has regained attention as an effective approach to upgrade biomass for energy supply.

2.1.2 Mechanisms of torrefaction

Lignocellulose is the main component of herbaceous and woody biomass, and includes lignin, cellulose and hemicellulose. Cellulose fibers are responsible for biomass being fibrous and

anisotropic. Hemicellulose, and lignin at a lesser degree, is mainly responsible for binding cellulose fibers together as shown in Figure 1. This structure can cause biomass to be resistant to comminution [19].

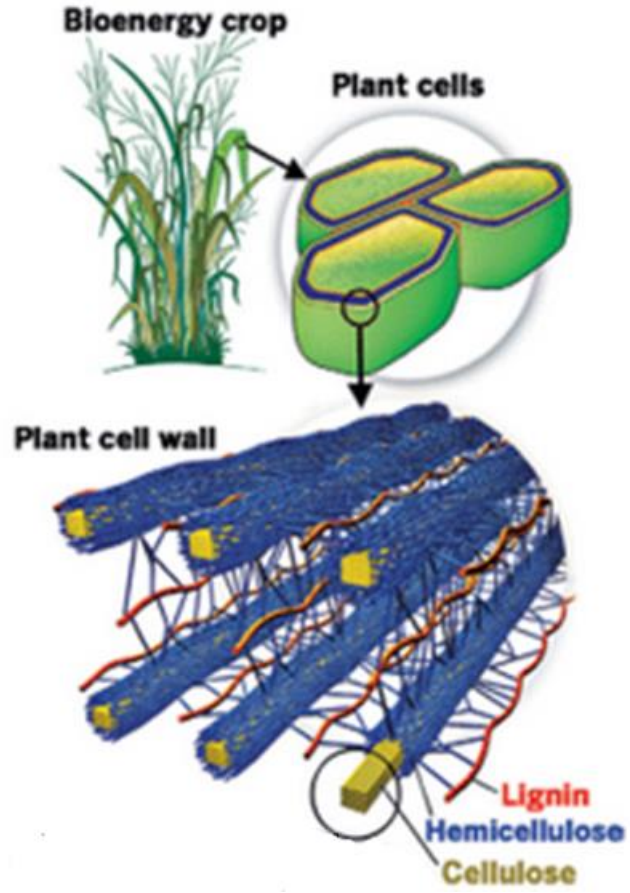

Figure 1. Lignocellulose structure. Adapted from *Biobased Society*, by A. Bruggink, 2013, retrieved from http://www.biobased-society.eu, Copyright 2013 by A. Bruggink. Adapted with permission.

Thermal decomposition of biomass under torrefaction conditions occurs via a complex group of reactions that convert lignocellulose and change the structure of the resulting solid. The reaction pathways are shown in Figure 2 [20].

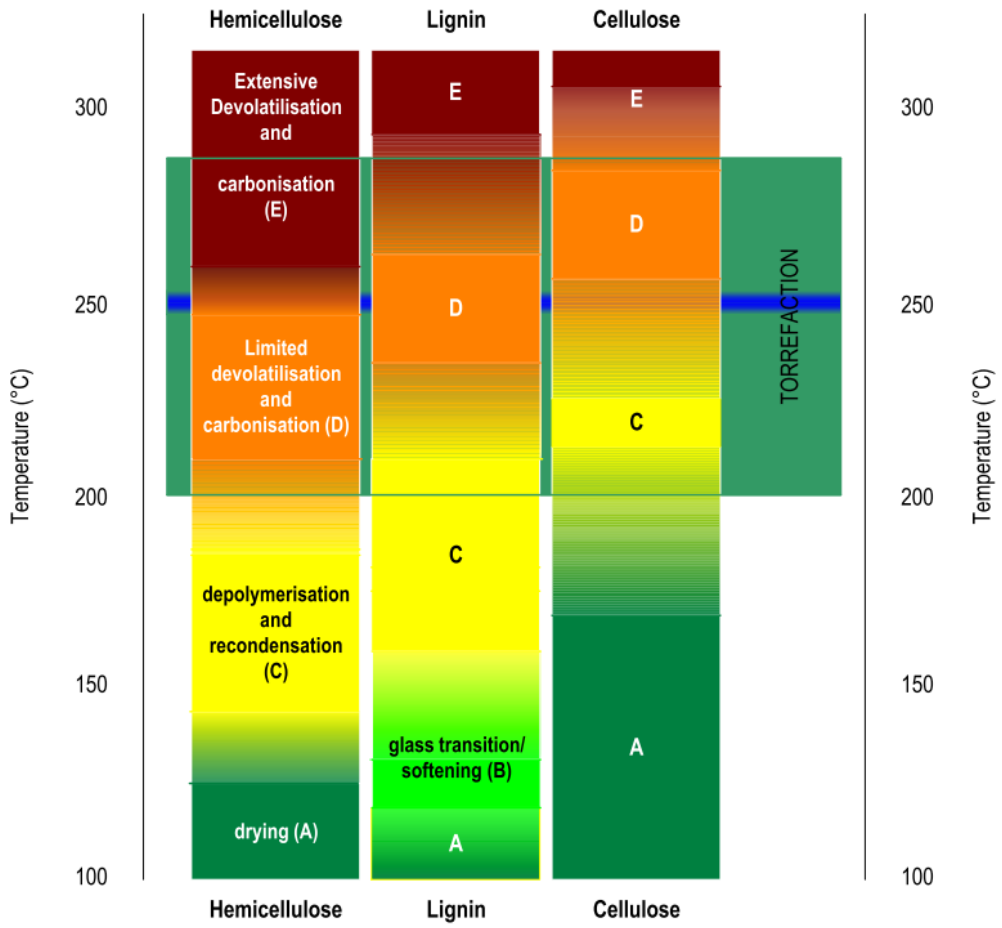

Figure 2. Reaction pathways during heating and torrefaction of lignocellulosic materials [20].

where the letters stand for:

A- physical drying

B- lignin softening

C- depolymerization and shortened polymers condensation

D- limited devolatilisation and carbonization

E- extensive devolatilisation and carbonization

Depolymerization and recondensation first occur on the hemicellulose fraction at about 140°C, while lignin is in the glass transition and softening phase and cellulose is being dried. Hemicellulose undergoes a very active reaction to the point of carbonization. Meanwhile, lignin and cellulose only partly undergo limited devolatilisation and carbonization. Accordingly, hemicellulose is the main contributor to the mass lost during biomass torrefaction [20].

Hemicellulose consists of shorter chains of 500 – 3,000 sugar units as opposed to 7,000 – 15,000 glucose molecules per polymer seen in cellulose. In addition, hemicellulose is a branched polymer, while cellulose is not branched. Different chemical structures affect the thermal thresholds for the various reaction pathways.

2.1.3 Torrefaction feedstock

Early research on torrefaction focused on wood-based material such as chips and sawdust. In 1984, Bourgois and Doat [21] torrefied four wood samples at 180°C, producing hydrophobic torrefied wood with high density and friability with about 90% energy yield. Later, Pentananunt et al. [22] studied upgrading of wood and sawdust briquettes by torrefaction. The products showed significantly less smoke emissions during combustion and a relatively faster rate of combustion. The mass and energy yields of the torrefied wood were66.7 – 83.3% and 76.5 – 89.6%, respectively. The corresponding values for sawdust briquettes were 76.3 – 93.8% and 83.1 – 95.3%, respectively.

During last ten years, torrefaction studies were focused on agricultural crops and agro-forestry residue. Literature for different torrefaction feedstock is summarized in Table 1 and selected experimental results are also included.

Table 1 – Mass yield, energy yield and higher heating value of torrefied biomass from literature (experimental results from selected literature).

Biomass	Related literature Ref.	selected Ref. for experiment	T (°C)	t (h)	Mass yield (wt.%)	Energy yield (wt.%)	HHV (MJ/kg)
Woody Biomass							
beech	[7], [14], [19], [23], [24]	[14]	280	0.5	73.8	88.1	18.3
eucalyptus	[21], [25–27]	[25]	270	0.5	67.6	75.2	22.8
			270	1.0	56.7	67.1	24.3
			290	0.5	50.6	67.3	27.3
larch	[7], [14], [19]						
lauan wood	[12]						
leucaena	[28]	[28]	200	0.5	91.0	94.1	21.0
			225	0.5	86.5	90.3	21.2
			250	0.5	73.0	76.2	21.2
			275	0.5	54.5	61.2	22.8
loblolly pine	[17], [29], [30]	[30]	250	1.3	83.8	89.7	21.0
			275	1.3	74.2	83.1	21.8
			300	1.3	60.5	73.2	23.6
pine	[11], [13]	[11]	225	0.5	89.0	93.9	19.5
			250	0.5	82.0	89.2	20.1
			275	0.5	73.0	86.3	21.8
			300	0.5	52.0	71.5	25.4
sawdust	[19], [31]	[31]	250	1.0	67.2	72.5	19.6
spruce	[23]						
willow	[7], [12], [19], [25], [32–34]	[25]	270	0.5	68.8	79.0	22.2
			270	1.0	67.5	79.2	22.8
			290	0.5	56.2	70.1	24.2
wood briquette	[19], [35]	[35]	250	1.0	65.0	71.6	22.1
Non-woody Biomass							
bagasse	[13], [31], [36]	[36]	230	1.0	87.5	96.4	17.1
			250	1.0	78.9	92.0	18.1
			280	1.0	68.6	82.9	18.7
bamboo	[12]						
coconut shell	[12]						

Biomass	Related literature Ref.	selected Ref. for experiment	T (°C)	t (h)	Mass yield (wt.%)	Energy yield (wt.%)	HHV (MJ/kg)
cotton stalk	[10]	[10]	250	0.5	33.8	45.3	24.6
empty fruit bunches	[9]	[9]	250	1.0	37.0	38.4	17.7
kernel shell	[9]	[9]	250	1.0	73.8	71.2	19.1
lucerne	[13]	[13]	250	1.0	81.6	83.1	18.8
mesocarp fiber	[9]	[9]	220	1.0	63.1	61.2	19.0
miscanthus	[32]	[32]	240	1.0	87.2	89.9	21.4
rape stalk	[37]	[37]	200	0.5	63.3	65.8	19.5
			250	0.5	38.3	41.0	20.1
			300	0.5	25.3	29.1	21.6
reed canary grass	[34]	[34]	250	0.5	83.0	85.1	20.0
			270	0.5	72.0	76.8	20.8
			290	0.5	61.5	68.8	21.8
rice husk	[31]	[31]	250	1.0	77.5	86.0	15.9
			270	1.0	74.3	83.3	16.1
			300	1.0	58.3	71.6	17.8
rice straw	[7], [19], [33], [37]	[37]	200	0.5	59.8	60.0	17.2
			250	0.5	40.3	42.5	18.0
			300	0.5	36.6	39.9	18.7
straw pellet	[13]	[13]	230	1.0	95.0	95.5	17.9
			250	1.0	90.0	92.1	18.2
			280	1.0	79.9	89.9	20.0
water hyacinth	[31]	[31]	250	1.0	78.5	96.1	12.7
			270	1.0	77.0	98.5	13.3
			300	1.0	70.0	95.0	14.1
wheat straw	[10], [34], [38]	[10]	200	0.5	47.6	56.0	19.8
			250	0.5	41.2	51.1	20.9
			300	0.5	31.6	40.7	21.7

2.1.4 Mass yield, energy yield and mass and energy balances

Two of the most important parameters in evaluating a torrefaction process are the mass and energy yields. An initial drying stage will remove any moisture in the biomass. The mass yield is based on mass loss after drying is completed. Between 200 – 300 °C, dehydration and devolatilisation of hemicellulose is the main contributor to mass loss [3].

The exact yield values for residue/ gas are strongly dependent on torrefaction temperature and biomass composition. Woody biomass typically retains 70% of the original mass as solid product and 90% of the initial energy content after torrefaction. Therefore, 30% of the original mass and nearly 10% of the chemical enthalpy is converted into torrefaction off-gas, carrying the energy as chemical or sensible enthalpy, see Figure 3. The energy densification ratio of torrefied biomass, which is defined as energy yield divided by mass yield, has atypical value around 1.3 [20].

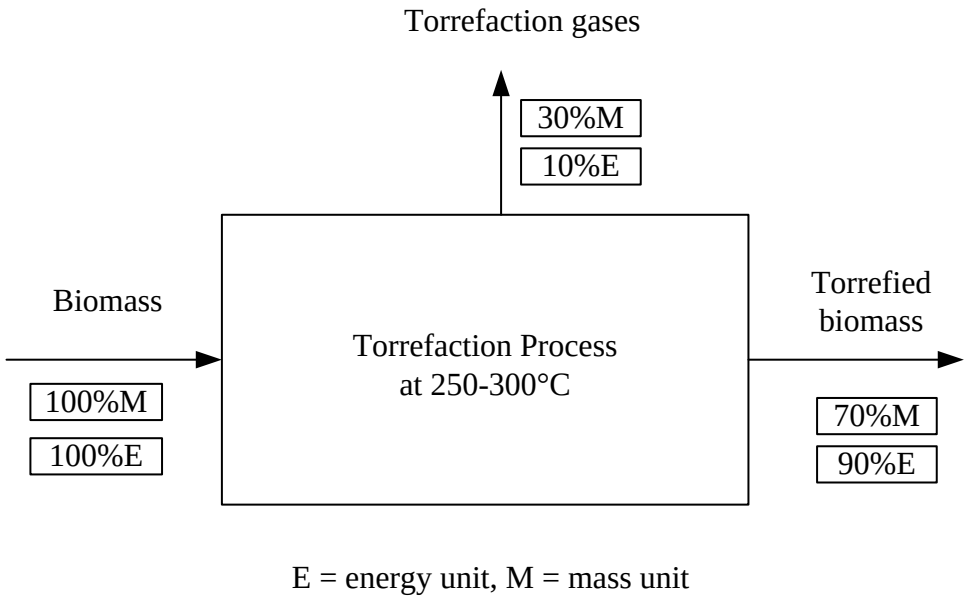

Figure 3. Typical mass/energy balance of torrefaction.

2.1.5 Ultimate and proximate analysis

Ultimate and proximate analysis are used to rank coals [39] and other solid fuels for suitability for combustion, gasification and pyrolysis.

Fixed carbon content substantially increases with increasing torrefaction temperature as shown in ultimate and proximate analyses. The lower loss of carbon from the feedstock, compared to oxygen and hydrogen, contributes to the increased heating value of the torrefied product [13,15,27]. Indeed, the elemental improvement, with regard to energy content, in biomass is an incentive for investigating torrefaction for biofuel applications. The Van Krevelen diagram shown in Figure 4 provides information about the elemental carbon, hydrogen and oxygen composition of various fuels. The atomic hydrogen to carbon ratio (H/C) is plotted against the atomic oxygen to carbon ratio (O/C). The differences in atomic ratios between untreated biomass and several typical solid fuels i.e. peat, lignite, coal are shown. Torrefied biomass has a lower O/C and H/C ratio, which is closer to coal.

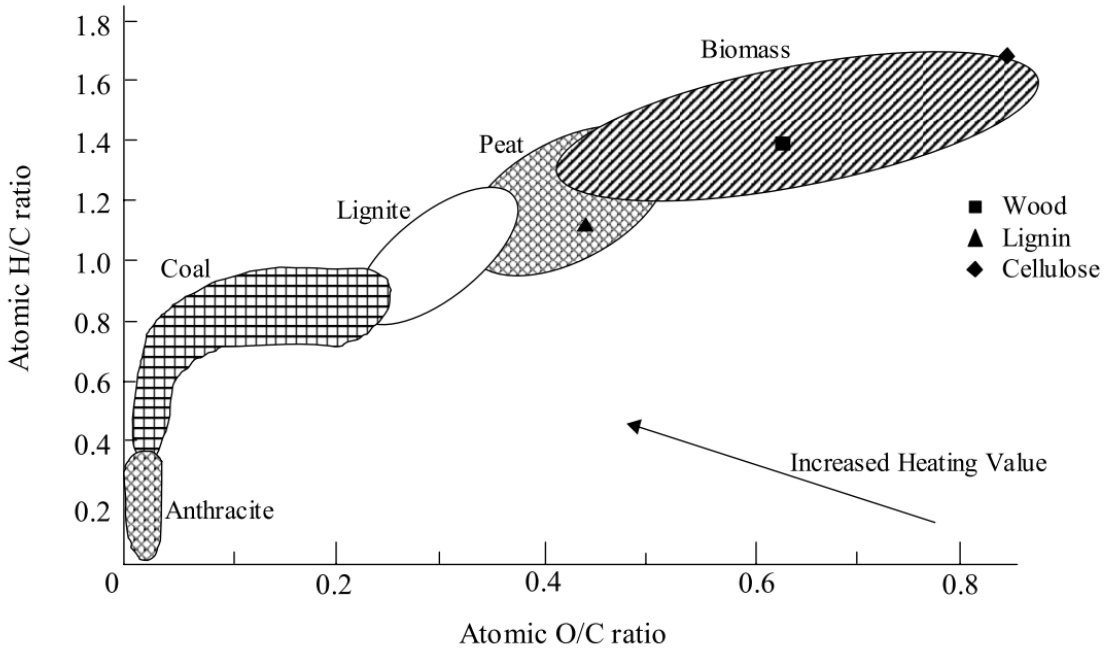

Figure 4. Van Krevelen diagram [14].

As torrefaction temperature and residence time increases, fixed carbon content increases while volatile content decreases. Consequently, the lower heating value (LHV) increases and the product becomes more energy dense [14,28]. The decomposition of oxygen from functional groups has been identified as responsible for this change. According to Chew's research [3], the loss of volatile matter from wheat straw, rice husk, logging wood chips, pine and sugarcane bagasse is around 25%, which is comparatively higher than other typical biomass, e.g. willow (5%), eucalyptus (10%), or leucaena (12%). Torrefaction causes an increase in ash content, incrementally 0.2% for leucaena to 10% (absolute) in rice husk. Increases of fixed carbon content are much higher, ranging from 0.9% for rice husk to 26.0% for leucaena.

2.2 Grindability

The grindability of a material is a measure of its resistance to crushing. The quantification of the grindability of solids, in this case coal and (torrefied) biomass, is essential in evaluating the practicability of size reduction of (torrefied) biomass in existing pulverized coal combustion fuel preparation systems. During the torrefaction process, the decomposition of hemicellulose weakens the viscous and elastic characteristics of woody cell wall, and the depolymerization of cellulose and thermal softening of lignin may also contribute in weakening the cell wall in vegetative material [33]. As a result, grindability of biomass can be improved by torrefaction, which reduces the energy requirements and costs for particle size reduction as well as milling equipment wear and tear [8, 16]. Torrefaction may also make it possible to use torrefied biomass in pulverized coal combustion systems without modification of existing coal mills [8].

The increased brittleness introduced by torrefaction improves the grindability of biomass. The accessibility of comminution in torrefaction studies is examined through the particle size distribution of milled samples. Generally, torrefaction results in improved grindability and grindability increases with the severity of the torrefaction conditions, i.e. increasing torrefaction temperature. Quantifying grindability improvements are discussed below.

The standard Hardgrove Grindability Index (HGI) used to analyze the grindability of coal has been studied in the literature for torrefied biomass samples [32]. HGI is determined through a multi-step procedure according to the ASTM standard method D409M – 09 [40]. A summary of the method is:

1. Acquire 50g of coal sample prescreened to particle sizes between 0.6 – 1.18mm.
2. Place the 50g sample in a ball mill. (The mill consists of a stationary grinding bowl with

a machined circular track. A loaded ring is placed on top of the set of milling balls with a fixed load of 29kg. A counter assembly automatically stops the ball mill after 60 revolutions.)

3. Crush the sample in the ball mill with eight 25.4 mm polished steel balls for 60 revolutions with a fixed load of 29 kg.
4. Classify the resulting milled sample and quantity material passing a #200 sieve (75μm).
5. Record and calculate the HGI value.

The HGI value is calculated from a regression equation obtained using four standard coals with known HGI values. The more material that passes the #200 sieve, the higher the HGI value and the easier it is to grind the parent material. A material that is difficult to grind has a low HGI value.

A modified HGI study adopted volumetric measurement for the sample to be milled in place of mass measurement, as biomass has lower bulk density compared to coal. As with the ASTM HGI method, the torrefied biomass and its parent materials were compared to milled coals of known HGI values by plotting the percentage of the sample that passed through a 75μm sieve against the known HGI values. A linear fit calibration curve can be used to determine the HGI values of the tested biomass. The equation determined by Ibrahim et al. [25] is given below:

$$\mathrm{HGI}_{\mathrm{equiv}} = \frac{\mathrm{m} + 11.205}{0.4955} \tag{3}$$

where *m* is the mass percentage of material passing a #200 sieve.

For extended torrefaction treatment temperature and duration, the treated biomass samples achieve similar grindability qualities as the reference coal samples. Literature indicates, however, that volumetric HGI may underestimate the grindability of biomass as a sizable fraction of the biomass is removed in the pre-milling step [32]. HGI requires pre-grinding of the coal, and only the coarsest particles from this step are used in a ball mill to evaluate the grindability. Consequently, the HGI may be based on that part of the coal that is most difficult to grind. It has been observed that, from the initial amount of torrefied biomass used, only a very small fraction of coarse particles was produced, which is much smaller compared to coal samples. This implies that a larger fraction of the initial mass was ground to a very small size, which would not limit the capacity of the coal mill. The grindability of torrefied biomass in terms of the HGI is thus improved after torrefaction, but commonly is still lower than HGI values of various coals [7]. According to Ibrahim et al.'s study of willow, softwood, eucalyptus and hardwood in 2012 [25], all the untreated biomass have a HGI value lower than 32 and torrefaction improved the grindability as the process conditions became more severe [24].

An alternative method of quantifying grindability couples the particle size distribution after grinding with the grinding energy consumption [3,8,11,16,31]. Generally, the specific energy consumption of the grinding machine is measured using a Wattmeter. The meter is connected to a data logging system and the energy consumption can be integrated over time. By recording the consumed electrical power during grinding via numerical Wattmeter, total grinding energy is evaluated by integration of the instantaneous power curve over the grinding period duration. Phanphanich & Mani [11] concluded that increasing torrefaction temperature was linearly correlated with decreasing specific grinding energy consumption for torrefied biomass, and that torrefaction could reduce energy consumption for grinding biomass by as much as 10 times [11].

Repellin et al. [23,42] observed a two stage mechanism. At lower temperature, dehydration and physical transformation of lignin improve the grindability. At the second stage, the thermal degradation of the cell wall contributes additional particle size reduction, leading to a higher percentage of fine particles after torrefaction. They also studied the relation between ball mill grinding energy and anhydrous weight loss (AWL), i.e. the torrefaction weight loss based on a bone dry sample. As the AWL of beech sample increased from 0 (no treatment) to 8%, grinding energy (kWh/Mg) decreased rapidly. Increasing AWL values beyond 8% resulted in diminishing reductions in grinding energy for the additional mass loss. To include a quantitative indicator of particle size reduction, a discriminatory criterion, *G*, was defined as the ratio between the grinding energy and the volumetric fraction of particles less than 200μm. Results of torrefied beech and spruce were given in Figure 5.

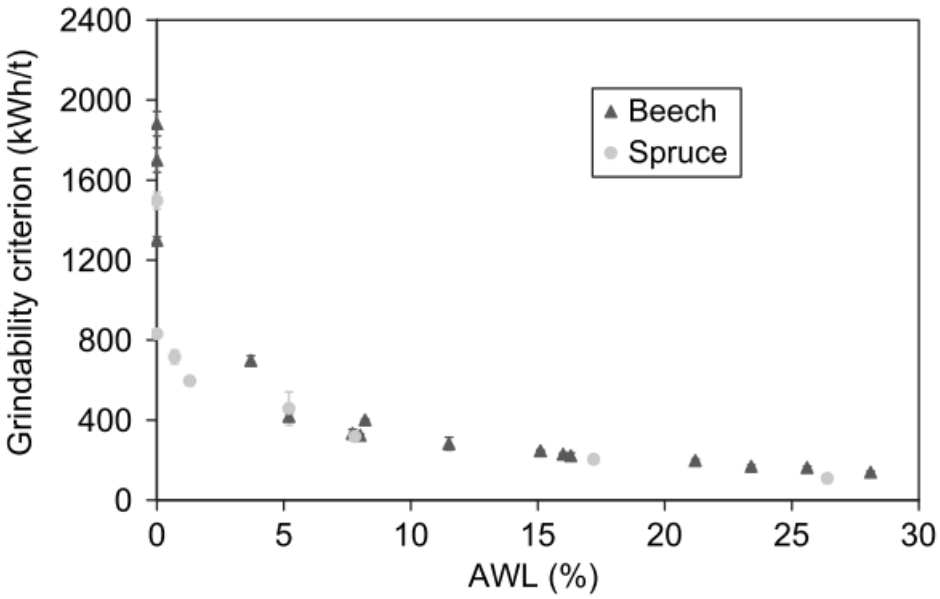

Figure 5. Grinding criterion (G) as a function of anhydrous weight loss (AWL) for beech and spruce. Reprinted from “Energy requirement for fine grinding of torrefied wood,” by V.

Repellin, A. Govin, M. Rolland, and R. Guyonnet, 2010, Biomass and Bioenergy, 34, vol. 34, no. 7, pp. 923–930. Copyright 2010 by Elsevier Ltd [42].

According to Reppellin's description of the above figure, G for spruce torrefied at 260°C for 5 min, is 4.7 times lower than G of natural wood. When the torrefaction condition is changed to 300°C for 5min, G is reduced by a factor of 13 – 14 compared with natural wood.

2.3 Equilibrium moisture content studies

The moisture content of biomass is of significant concern during thermo chemical conversion, e.g. combustion, gasification, or pyrolysis. In combustion, energy is required to evaporate moisture, potentially reducing overall system efficiency and resulting in incomplete combustion and higher emissions of CO, unburned hydrocarbons, SO_2, and NO_x. Limited moisture is also advantageous in gasification. The steam generated can increase the hydrogen yield of the product gas via water gas shift reactions and enhance carbon conversion; however, too much moisture will require a dryer, increasing total costs. In pyrolysis, the existence of moisture increases char formation. The yield of tar, on the other hand, can either be suppressed or increased by the presence of water in the feedstock based on pyrolysis temperature and ash content [43]. Indeed, improving the hydrophobicity of biomass materials by torrefaction can provide additional benefits to justify its use as a pretreatment process. Reducing moisture content and increasing hydrophobicity can be a clear advantage for biomass conversion logistics by reducing covered storage requirements and reducing the weight of materials for transportation.

The hydrophobic property of torrefied biomass may be examined via: (a) an immersion test, or (b) an equilibrium moisture content (EMC) study.

In an immersion test, treated and untreated biomass samples are submerged in water for a fixed time. Comparing the final moisture content of materials after immersion provides an indicator of hydrophobicity [29,35].

To measure the EMC value, a biomass sample is exposed to an environment with constant humidity and temperature until the moisture in the biomass reaches an equilibrium value. An aqueous saturated salt solution is used to keep the environment at a constant relative humidity. By using various salts solutions, the relative humidity can be adjusted over a wide range (0–100%) [17].ASTM E104 – 02 (2012) [44] provides guidelines for humidity fix point (HFP) salts and the corresponding acceptable temperature ranges as shown in Table **2**.

Table 2 – Humidity fix point (HFP) salt solutions. Note that XX in HFP XX in column 1 is the relative humidity.

HFP Designation	Salt Name	Chemical Symbol	Temperature Range (°C)
HFP 4	Cesium fluoride	CsF	15 to 80
HFP 7	Lithium bromide	LiBr	5 to 80
HFP 12	Lithium chloride	LiCl	5 to 80
HFP 23	Potassium acetate	CH_3COOK	10 to 30
HFP 33	Magnesium chloride	$MgCl_2$	5 to 80
HFP 43	Potassium carbonate	K_2CO_3	5 to 30
HFP 59	Sodium bromide	NaBr	5 to 80
HFP 70	Potassium iodide	KI	5 to 80
HFP 75	Sodium chloride	NaCl	5 to 80
HFP 85	Potassium chloride	KCl	5 to 80
HFP 98	Potassium sulfate	K_2SO_4	5 to 50

Greenspan [45] provided the EMC values of selected saturated salt solutions from 0–40°C as shown in Table 3.

Table 3 – Equilibrium relative humidity of selected saturated salt solutions from 10 to 40 °C.

Relative Humidity, % \ T,°C	10	15	20	25	30	35	40
Cesium Fluoride	4.9	4.3	3.8	3.4	3.0	2.6	2.4
Lithium Bromide	7.1	6.9	6.6	6.4	6.2	6.0	5.8
Zinc Bromide	8.5	8.2	7.9	7.8	7.6	7.6	7.5
Potassium Hydroxide	12.0	10.7	9.3	8.2	7.4	6.7	6.3
Sodium Hydroxide		9.6	8.9	8.2	7.6	6.9	6.3
Lithium Chloride	11.2	11.3	11.3	11.3	11.3	11.3	11.2
Calcium Bromide	23.6	20.2	18.5	16.5			
Lithium Iodide	20.6	19.6	18.6	17.6	16.6	15.6	14.6
Potassium Acetate	23.4	23.4	23.1	22.5	21.6		
Potassium Fluoride				30.9	27.3	24.6	22.7
Magnesium Chloride	33.5	33.3	33.1	32.8	32.4	32.1	31.6
Sodium Iodide	41.8	40.9	39.7	38.2	36.2	34.7	32.9
Potassium Carbonate	43.1	43.2	43.2	43.2	43.2		
Magnesium Nitrate	57.4	55.9	54.4	52.9	51.4	49.9	48.4
Sodium Bromide	62.2	60.7	59.1	57.6	56.0	54.6	53.2
Cobalt Chloride				64.9	61.8	58.6	55.5
Potassium Iodide	72.1	71.0	69.9	68.9	67.9	67.0	66.1
Strontium Chloride	75.7	74.1	72.5	70.9	69.1		
Sodium Nitrate	77.5	76.5	75.4	74.3	73.1	72.1	71.0
Sodium Chloride	75.7	75.6	75.5	75.3	75.1	74.9	74.7
Ammonium Chloride	80.6	79.9	79.2	78.6	77.9		
Potassium Bromide	83.8	82.6	81.7	80.9	80.3	79.8	79.4
Ammonium Sulfate	82.1	81.7	81.3	81.0	80.6	80.3	79.9
Potassium Chloride	86.8	85.9	85.1	84.3	83.6	83.0	82.3
Strontium Nitrate	90.6	88.7	86.9	85.1			
Potassium Nitrate	96.0	95.4	94.6	93.6	92.3	90.8	89.0
Potassium Sulfate	98.2	97.9	97.6	97.3	97.0	93.7	96.4
Potassium Chromate				97.9	97.1	96.4	95.9

Test samples attain an equilibrium moisture state when the measured weight is constant for a targeted duration. Hence, it is possible to examine the effect of torrefaction on equilibrium moisture content over a large range of humidity to simulate different storage conditions. Moisture content on a wet and dry basis is defined below.

Wet-basis moisture content, MC_W:

$$\mathrm{MC_W} = \frac{\mathrm{G_W} - \mathrm{G_D}}{\mathrm{G_W}} \times 100\% \quad (4)$$

Dry-basis moisture content, MC_D:

$$\mathrm{MC}_D = \frac{G_W - G_D}{G_D} \times 100\% \quad (5)$$

where:

G_W is mass of wet material

G_D is mass of dry material (determined by the oven method specified in ASTM E871 [46] ASAE S352.2)

Numerous models have been proposed, including semi-theoretical, semi-empirical, and empirical models. Van den Berg and Bruin [47] reviewed 77 isotherm models for biological materials, including wood and other fibrous materials. The American Society of Agricultural Engineers [48] adapted modified Chung-Pfost, Modified Henderson, Modified Halsey, and Modified Oswin models as standard models for fitting EMC experimental data [49]. Isotherm equations and equation constants were provided for the moisture relationship of plant – based agricultural materials and their products.

Modified Henderson Equation:

$$\mathrm{RH} = 1 - \mathrm{e}^{[-\mathrm{A}*(\mathrm{T}+\mathrm{C})*(\mathrm{MC_D})^{\mathrm{B}}]} \quad (6)$$

The Modified Henderson model is based on the Gibbs' thermodynamic adsorption equation.

Modified Chung-Pfost Equation:

$$\mathrm{RH} = \mathrm{e}^{\left[-\frac{\mathrm{A}}{\mathrm{T}+\mathrm{C}}*\mathrm{e}^{(-\mathrm{B}*\mathrm{MC_D})}\right]} \quad (7)$$

The assumption of the Chung-Pfost model is that moisture content is related to the free energy for sorption.

Modified Oswin Equation:

$$\mathrm{RH} = [(\frac{\mathrm{A}+\mathrm{B}*\mathrm{T}}{\mathrm{MC_D}})^{\mathrm{c}} + 1]^{-1} \quad (8)$$

The Oswin model is a purely empirical, mathematical expression for sigmoid shaped curves.

where *RH* is the relative humidity (decimal); *T* is the temperature (ºC); MC_D is the dry-basis moisture content, *A, B* and *C* are the equation constants which can be checked in ASAE Standards D245.5 (Table 2 – Isotherm equation constants for agricultural products isotherm).

Besides the three models recommended by ASAE, a model proposed by Vasquezand Coronella (Vasquez-Coronella Sorption Mixing model) [50] has been applied to several data

sets. Bellur et al. [51] found that the VCSM model accurately describes the EMC of biosolids as the model incorporates effects such as mixing and swelling in addition to adsorption [49]. Vasquez and Coronella concluded that the model helps to explain some of the physical phenomena of water sorption in woody biomass [52]. This VSCM model is based on standard molecular thermodynamic approaches and statistical mechanics. In this model, three phases of water are in thermodynamic equilibrium: the water vapor in the surrounding air and the two phases of adsorbed water in the biomass: bonded, or strongly adsorbed, and free, or non-bonded. Water bonds strongly to the biomass through adsorption mechanisms. Non-bonded water refers to condensed water in the biomass phase that is absorbed to the biomass. Thus, the EMC of the biomass is the sum of the bonded water (θ) plus non-bonded water (α).

$$EMC = \alpha + \theta \tag{9}$$

At equilibrium:

$$\theta(\alpha+\theta)exp(\Delta\varepsilon) = \alpha(\sigma-\theta)exp(\Delta F) \tag{10}$$

$$(\alpha+\theta)HR = \alpha exp(\Delta F) \tag{11}$$

where $\Delta F = \ln(1-\phi_p) + \phi_p + \chi\phi_p{}^2 + \tilde{\upsilon_{pw}}\left(\phi_p{}^{\frac{1}{3}} - \phi_p{}^{\frac{5}{3}}\right)$

σ is an adjustable parameter that describes the adsorption capacity of the water bound phase

$\Delta\varepsilon$ is an adjustable parameter that characterizes the difference in molecular potential energy between water in the θ phase and that of pure water. χ is the Flory – Huggins interaction parameter; and$\upsilon_{pw}$is the average specific volume ratio of biomass to water in the biomass volumetric fraction used to find ϕ_p:

$$\phi_p = \frac{\tilde{\upsilon_{pw}}}{(\alpha + \theta) + \tilde{\upsilon_{pw}}} \quad (12)$$

$\phi_p$describes the relative volume of biomass to water in the Flory – Huggins framework [50].

The VSCM model was also reported to have some limitations and might be improved by accounting for additional molecular interactions and contributions such as pH, ionic conditions, and surface tension. Furthermore, introducing a better model in place of lattice structure (such as a stochastic distributed network) to describe biomass structure can improve this model [17,50].

2.4 Biological durability

Microbial decay is generally observed during storage of untreated, moist biomass, which can lead to problems such as degradation of biomass, moldiness and even fermentation. It is generally acknowledged that heat treated wood has better resistance against microbial decay [44 – 49].According to earlier research [49 – 51], the improved durability of heat-treated wood against fungi can be explained by three different reasons:

- The increase of hydrophobicity and a consequent reduction of the EMC value constrain the growth of microorganism.
- Hemicellulose, an easily available substrate for microbial organism, is greatly reduced in torrefied biomass as it decomposes readily during heat treatment of wood.
- Breakdown products of torrefied biomass include compounds such as furfural that can inhibit microbial decay.

Relevant literature related to wood decay, microbial growth, and degrading activities are summarized below. Petersen demonstrated that wood at a moisture content below 20% could inhibit fungi development [53]. Numerous studies have been done on the decay resistance of heat treated wood intended for building materials. Weight loss caused by fungal decay is monitored as an indicator of decay. Resistance to decay was found to be proportional to mass loss due to thermal treatment. Hemicellulose degradation occurs as a result of thermal treatment, and carbon content or O/C ratio can be used as an indicator of wood durability [60]. Hakkou et al. carried out thermal treatment of beech wood at 10 temperatures over a range from 20 to 280°C. The results showed a clear correlation between the temperature of treatment and the fungal durability [56].

The studies mentioned above mainly focused on a temperature range from 180 – 240°C, however torrefaction research should pursue complete durability data over a temperature range from 200 to 300°C. Besides, most decay studies used wood blocks as test samples [61], the information on durability of untreated and treated biomass in small particle sizes is very limited.

- **3. Thesis statement**

The following outlines the desired outcomes of this research.

- Evaluate the fuel performance of torrefaction over a range of temperatures for leucaena, energy cane, eucalyptus, sugarcane, sugar cane bagasse and banagrass by heating value test and ultimate analysis.
- Use a modified HGI method to evaluate the effects of torrefaction on the grindability of leucaena, energy cane, eucalyptus, sugarcane, sugar cane bagasse and banagrass.
- Determine the equilibrium moisture content of torrefied and untorrefied leucaena, energy cane, eucalyptus, sugarcane, sugar cane bagasse and banagrass as a function of relative humidity and assess the applicability of equilibrium moisture content model to the data.

- **4. Materials and Methods**

The following sections describe the materials and methods proposed for the torrefaction study.

4.1 Parent materials

Eucalyptus grandis was obtained from commercial plantations on the island of Hawaii, north of Hilo, belonging to GMO Renewable Resources LLC. *Leucaena leucocephela* samples were obtained from experimental plantings at the University of Hawaii's Waimanalo Experiment Station. Banagrass, a hybrid of napier grass (*Pennisetum purpureum*) and pearl millet (*Pennisetum glaucum*), energy cane (variety Molokai 6018), and commercial sugar cane were harvested from experimental plots on the Hawaiian Commercial & Sugar Co. (HC&S) plantation at Puunene, HI. HC&S was also the source of sugar cane bagasse, the fibrous byproduct of sugar manufacturing in their Puunene factory.

The two wood materials were harvested from standing trees and the bole wood/logs were chipped (Morbark, Model 10) and dried to ambient equilibrium moisture content (~10% dry basis moisture content) prior to use in torrefaction experiments. A sample of sugar cane bagasse was removed from the HC&S bagasse storage building and dried to ambient equilibrium moisture content prior to use in the torrefaction tests.

The banagrass, energy cane and sugar cane were hand harvested from plots and shipped to Honolulu. Each fuel lot was shredded with a laboratory scale shredder (Vincent Corporation, Model VCS-8). Each lot was divided in half, and one half was dried to ambient equilibrium moisture content after shredding (S0). The other half of each fuel lot was:

(1) dewatered using a screw press (Vincent Corporation, Model CP-4);

(2) rinsed in ambient tap water for one minute at a water to fiber ratio of 10:1;

(3) drained of free water for five minutes;

(4) dewatered a second time using the screw press from (1);

(5) dried to ambient equilibrium moisture content.

This treatment was designed to remove water soluble elements, primarily K and Cl, which are known to cause problems related to ash deformation and melting at temperatures typical of thermochemical conversion. The treated materials are referred to as S3 materials hereafter.

4.2 Torrefaction methods

The following sections describe the torrefaction methods employed in this study.

4.2.1 Torrefaction reactor

Figure 6 presents a schematic of a laboratory scale torrefaction unit. The fixed-bed reactor is made from a stainless tube (Di = 4.86 cm, length = 15.4 cm) capable of torrefying batch samples of around 50 gram. The reactor is placed inside Thermolyne F21100 Tube Furnace and a continuous flow of nitrogen controlled with a mass flow controller is directed through the reactor to maintain an inert environment and sweep volatile products from the reactor. A stainless steel screen at position 0cm holds the biomass.

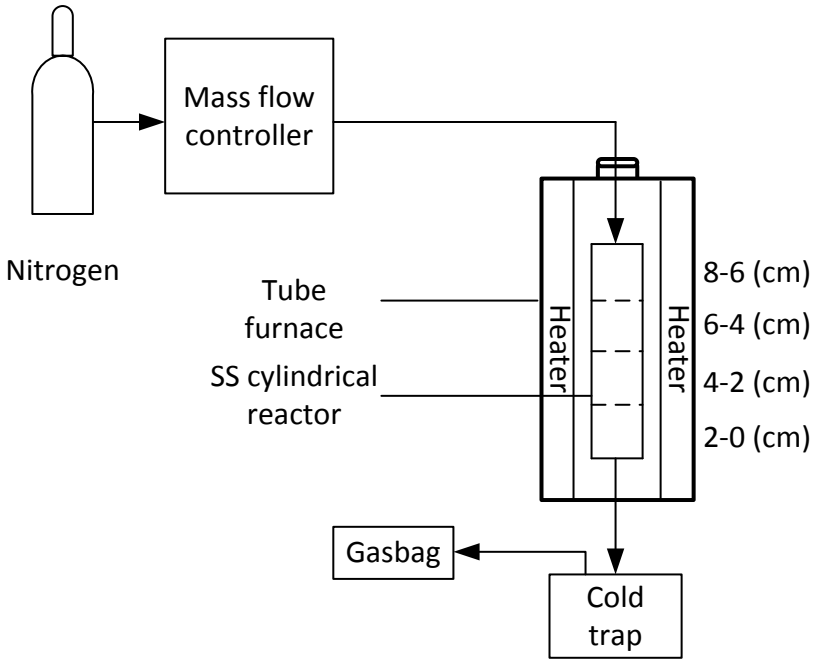

Figure 6. Schematic of first lab scale torrefaction unit.

Parent materials were analyzed by ultimate analysis (amounts of carbon, hydrogen, oxygen, sulphur, nitrogen, chloride and other impurities) and proximate analysis [62] (fixed carbon, volatile material [63], ash content [64] and moisture content [46]) by HazenResearch, Inc. Heating values of torrefied and parent biomass sample were also measured in the laboratory at HNEI with a Parr 6200 Bomb Calorimeter from Parr Instrument Company.

A Parr 6200 Bomb Calorimeter was used for the heating value measurement. The sample to be tested is electrically ignited in a stainless steel bomb filled with 30 bar of oxygen. The vessel is submerged into water and the heat released during combustion is calculated by measuring the change of temperature in the water bath.

Figure 7. Parr 6200 Bomb calorimeter and bomb (Photos from Parr Instrument Company).

Calorimeter Operation Summary:

Dry the untreated or torrefied sample in oven at 105°C for 24 h. Turn on the calorimeter and open the valve on the oxygen supply cylinder. Go to the Calorimeter Operation menu; turn on the Heater and Pump.

Tare a sample cup and weigh a sample of biomass into the sample cup to the nearest 0.001 g.

Figure 8. Cotton thread attached to the fuse wire.

Put the sample cup on the sample bomb cylinder head and attach a cotton thread to the fuse wire as shown in Figure 8. Load the head into the bomb cylinder and seal the cylinder.

Connect the oxygen supply cylinder to the bomb cylinder. Press the O_2 fill button on the Calorimeter Operation screen.

Position the bomb in the pail, and then position the pail in the calorimeter.

Attach the ignition wires to the terminals on the 1108P bomb head.

Fill the bucket with 2 liters of water at 25 – 27°C. Observe the bomb to make sure that there are no oxygen leaks. After this, close the lid making sure that neither the stirrer nor the bucket thermistor are touching the 1108P bomb or bucket.

Choose Standardization (calibration) or Determination (unknown samples) for Operating Mode.

Once the test results have been displayed, the calorimeter will be ready for the next test when the next sample is ready.

Open the lid and remove the bucket with the bomb. Remove the 1108P bomb from the bucket and release the pressure by loosening the valve knob. Rinse the bomb head and cylinder. Dry the bomb head, cylinder and screw cap.

The bomb is now ready to prepare for the next test.

4.2.2 Preliminary test

Nitrogen flow rate was set at about 1.2 L/min from top to bottom of the tube reactor. At position 0cm (bottom) there was a stainless steel screen to hold the biomass. 50g leucaena with

moisture content of 9.5% (wet basis) was tested. The oven temperature was first set to 120°C to allow for drying for 100min. Then the temperature was set to 260°C at a 10K/min ramping rate to achieve torrefaction. After 60 min of torrefaction, the oven was turned off while still flushing with N_2 until biomass temperatures were below 100°C.In two preliminary torrefaction tests of sample size around 50g, the heating values of torrefied samples produced at different locations along the vertical axis of the reactor were evaluated. The locations are divided by four sections with each length of 2cm, from bottom to top of the tube reactor as shown in Figure 6. After processing heating value measurement described in 4.2.1 Torrefaction reactor, data presented in Table 4 show that the location in the reactor has a strong influence on the heating value of the product. Average heating values range from 18.2 to 24.6 MJ kg^{-1}.

The results of first test on 5-27-2013 are shown in Table 4**.**

Table 4 – Results of preliminary torrefaction test 1: HHV of torrefied leucaena with final torrefaction temperature of 260 °C as a function of reactor tube position.

Position from bottom(cm)	Run 1 (MJ/kg)	Run 2 (MJ/kg)	Run 3 (MJ/kg)	Run 4 (MJ/kg)	Mean (MJ/kg)	Standard deviation
8 – 6	18.56	18.45	17.49		18.17	0.59
6 – 4	18.72	22.917	22.88	20.38	21.22	2.05
4 – 2	22.69	22.59	21.14		22.14	0.87
2 – 0	24.56	24.95	24.24		24.58	0.36

The second test, conducted on 6-3-2013, differed in that the maximum oven temperature was set to 220°C (instead of 260°C) and the position in the tube furnace was offset 1 cm. Results are shown in Table 5:

Table 5 – Results of preliminary torrefaction test 2: HHV of torrefied leucaena with final torrefaction temperature of 220 °C as a function of reactor tube position.

Position from bottom(cm)	Run 1 (MJ/kg)	Run 2 (MJ/kg)	Run 3 (MJ/kg)	Mean(MJ/kg)	Standard deviation
9 – 7	24.31	19.75	19.95	21.34	2.58
7 – 5	22.07	22.07	21.17	21.77	0.52
5 – 3	27.95	26.94	27.07	27.32	0.55
3 – 0	27.09	27.85	27.21	27.38	0.41

For the second test, the appearances of torrefied samples from four different locations in the reactor are shown in Figure 9. Samples generated in the 5 – 3cm and 3 – 0 cm locations don't show macroscopic differences. The sample generated in the 7 – 5 cm location was less brittle to the touch and the one from the 9 – 7 cm location appeared to be brown in color compared to the others, which were dark black.

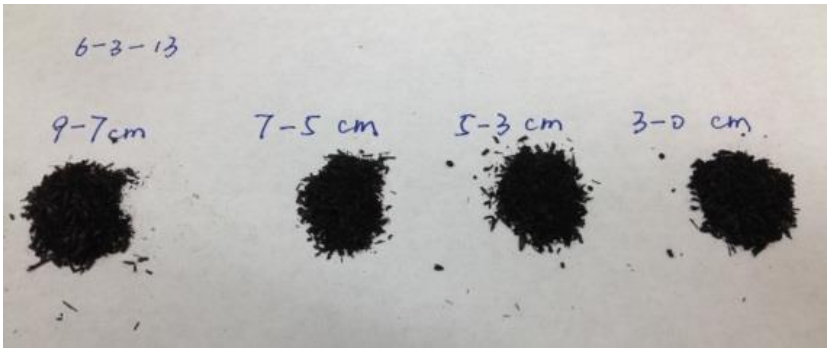

Figure 9. Appearance of torrefied leucaena in test 2.

4.2.3 Pan shape reactor

To obtain better uniformity of torrefaction results, a pan shape reactor was built by Dr. Tim Petrik. Instead of the tube furnace design, the shallow fuel bed in the reactor was heated in a

muffle furnace (Isotemp® Programmable Muffle Furnace 650 – 750 Series). The schematic of second torrefaction unit is shown in Figure 10.

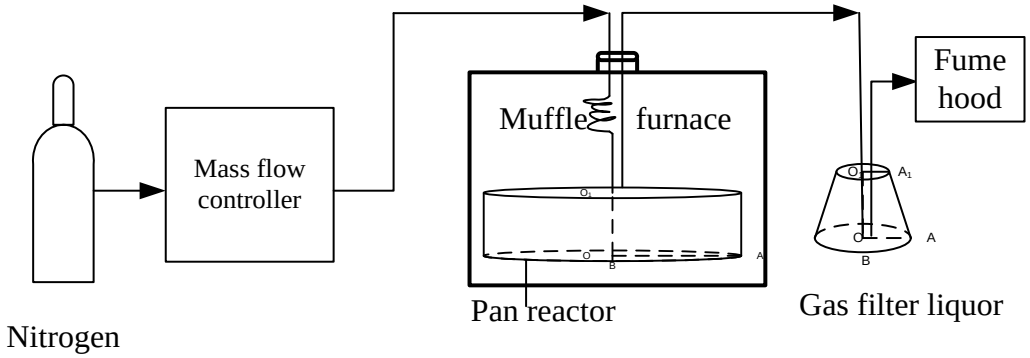

Figure 10. Schematic of second torrefaction unit.

Table 6 – HHV of torrefied leucaena samples from different positions in the pan-shaped torrefaction reactor.

Position(cm)	Run 1 (MJ/kg)	Run 2 (MJ/kg)	Run 3 (MJ/kg)	Mean (MJ/kg)
6-Top	17.18	14.00	17.43	17.31
6-Bot	14.73	16.95		16.95
M-Top	17.19	16.84		17.02
M-Bot	16.36	N/A	17.71	17.04
12-Top	15.93	16.82		16.38
9-Top	17.03	17.00		17.02
3-Top	17.49	15.27		17.49
			STDEV:	0.35

Test results using the pan reactor are shown in Table 6. Seven locations were sampled. Samples taken from the 3, 6, 9 and 12 o'clock positions of the pan reactor correspond to the 3, 6, 9, and 12 designations in Table 6. "M" stands for the center of the pan reactor. "Top" is located at a depth of 1 cm from the top of the torrefied layer, and "Bot" is located at the bottom of the torrefied leucaena layer in the reactor. Samples 6-Top Run 2 and 6-Bot Run 1 had small sample

weights (<0.25g, whereas the others were around 0.4g) and that may be the reason their heating values were low. Material from Sample 3-Top Run 2 was displaced from the sample cup during the calorimeter measurement and did not completely combust.

The standard deviation of the HHV measurements from seven locations in the pan shaped reactor was ~2% of the mean measured value (for all runs at all locations) indicating that the product of the torrefaction process had good spatial uniformity.

The capacity of the pan shape reactor is around 30g; however, 80 grams per batch are required to determine grindability, hydrophobicity and microbial decay. The reactor shape was therefore redesigned from round to square and 5cm of depth was added. The dimensions of the square pan are 25.5cm×25.5cm. About 150g chopped biomass (<2 mm particle size) can be torrefied per batch with the new reactor.

Figure 11. Square torrefaction reactor.

Results of tests to assess the uniformity of the torrefied biomass produced by the square reactor are shown in Figure 12. Values shown in the figure, upper pair: A(B); and lower pair: C(D), are the average higher heating values in MJ kg^{-1} (A and C) and standard deviations (B and D). A and B are based on samples located at a depth of 2 cm from the top of the torrefied layer.

Similarly, C and D are based on samples taken at the bottom of the torrefied layer in the reactor. In total, ten positions were sampled in triplicate for the uniformity test**.**

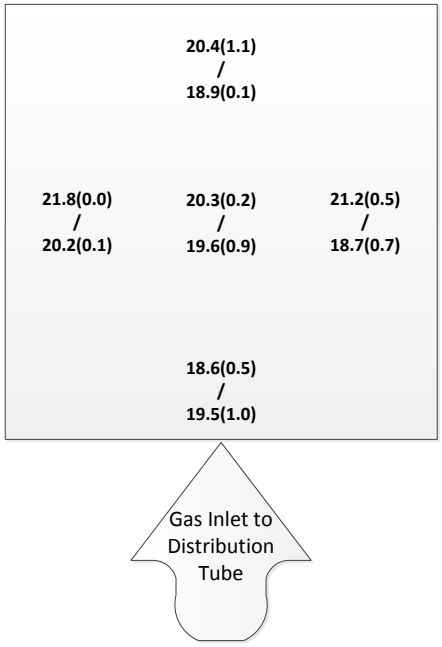

Figure 12. Average higher heating values of torrefied leucaena at different positions in the square (25.5cm x 25.5cm) reactor.

After preliminary tests to assess the uniformity of the torrefaction treatment using the square reactor were completed, the parent materials described in section 4.1 were torrefied at muffle furnace controller set point temperatures of 220, 250, 270, 300, and 330°C.

4.3 Grindability Test design

The modified Hardgrove Grindability Index method proposed by Bridgeman et al. [32] was adopted for the grindability study in this investigation. The modified method is based on ASTM

D409-2009, “Standard Test Method for Grindability of Coal by the Hardgrove Machine Method” [65]. Bridgeman et al. adapted the ASTM method for coal to biomass. The main differences included using a ball mill instead of the ASTM D409 mill and, to accommodate the lower bulk density of biomass compared to coal, a sample size of 50 mL was employed instead of the 50g used in ASTM D409.

4.3.1 Preparation of test samples

As reported by previous research [25,30], HGI values of untreated biomass fuels are usually much lower than 40.Standard reference coal materials with low HGI values of 27, 47, 64, and 89 were obtained from the Australian Coal Preparation Society’s (ACPS) CHOICE Analytical Pty Ltd.

To prepare the 1.18mm×600μm (screen sizes No. 16 × No. 30) test sample, 1 kilogram of an air-dried standard reference coal with known HGI was comminuted with a cutting mill (PULVERISETTE19, FRITSCH) fitted with a 4.75mm (No. 4) outlet screen. Samples were fractionated according to size in lots no greater than 250g for 5 minutes in a mechanical sieving machine (RX-29, W. S. Taylor Inc.) using a set of nested sieves containing a 1.18mm (No. 16) sieve on top of a 600μm (No. 30) sieve to obtain the size fraction required by the test method [65].

4.3.2 Ball mill description

Grinding the fuels for the modified HGI test was accomplished using a ball mill (Model PM100, Retsch). A 500mL stainless steel jar with 25, 20mm diameter balls was used for the sample treatment.

Figure 13. Retsch PM 100 ball mill, milling jar and milling balls (Photos from Retsch Company).

Preliminary milling tests were conducted using coal, biomass, and torrefied biomass in order to determine the suitable operating conditions for the torrefied material. The mill was then calibrated with standard reference coals to allow a comparison between the fuels.

4.3.3 Calibration

Calibration of the modified HGI measurement is described below. 50cm^3 of each fractionated (1.18mm×600μm) standard reference material coal was measured and weighed using a graduated

cylinder and a balance accurate to ±0.1g. The 50cm^3 sample was placed into a 500 mL capacity stainless steel milling cup with 25, 20mm stainless steel balls and milled for 2 min at 165 rpm. The resulting sample was removed from the grinding cup and separated using a 75 µm sieve and a sieve shaker for 5 min. The two resulting fractions were weighed to the nearest 0.01 g. If a loss of sample greater than 0.5 g was recorded (sum of the two size fraction weights minus initial weight), the test was aborted and repeated. The percentage of sample that passed through the 75 µm sieve is calculated using:

$$m = (m_v - m_1) / m_v \tag{13}$$

where:

m = percentage of sample that passed through the 75 µm sieve

m_v = mass of 50 cm^3 sample

m_1 = mass of sample collected on 75 µm sieve.

This process is repeated three more times and an average value of the four results is calculated and repeated for each of the four standard reference material coals with HGI values of 27, 47, 64, and 89.The results were used to plot a calibration curve for HGI versus *m*. Using the least square method, an equation for the linear fit of the data from the standard reference coal was obtained. The equation of the line for the sum of least squares takes the form of:

$$\mathrm{Y = a + bX} \tag{14}$$

where:

Y=HGI,

a= y axis intercept,

b= slope of the regression line, and

X= material mass that passed through the 75µm (No.200) sieve.

a and b can be determined by use of the following and equations

$$a = \frac{\sum Y \sum X^2 - \sum X \sum XY}{n\sum X^2 - \left(\sum X\right)^2} \tag{15}$$

$$b = \frac{n\sum XY - \sum X \sum Y}{n\sum X^2 - \left(\sum X\right)^2} \tag{16}$$

4.3.4 Test of biomass fuel

Parent feedstocks and torrefied fuels samples were analyzed using the steps outlined above in Section 4.2.3 for calibration, with all results produced in three replicates. The mass in grams passing through the 75 µm sieve was entered into the regression equation determined from the calibration curve and a HGI value was calculated for each biomass fuel.

To provide a more thorough assessment of the grindability behavior of the torrefied fuel in comparison to coal, a particle size distribution of the ground fuels was also determined. The fuels were sieved with a series of sieves of mesh sizes 600, 425, 212, 150, 75 and 53 µm. The mass of sample collected on each sieve was measured and recorded as a percentage of the original sample mass. A plot of the particle size distribution of each ground sample was made using the midpoint between two consecutive sieve sizes as the particle size for each size class (e.g. the particle size of a sample collected on the 425µm sieve was assumed to be 512.5µm). The particle sizes of thermally treated biomass were plotted alongside those of the four HGI standard

reference coals to compare their behavior. A figure from Femi Akinrinola and Dr. Leilani I. Darvell, University of Leeds [66] is presented below:

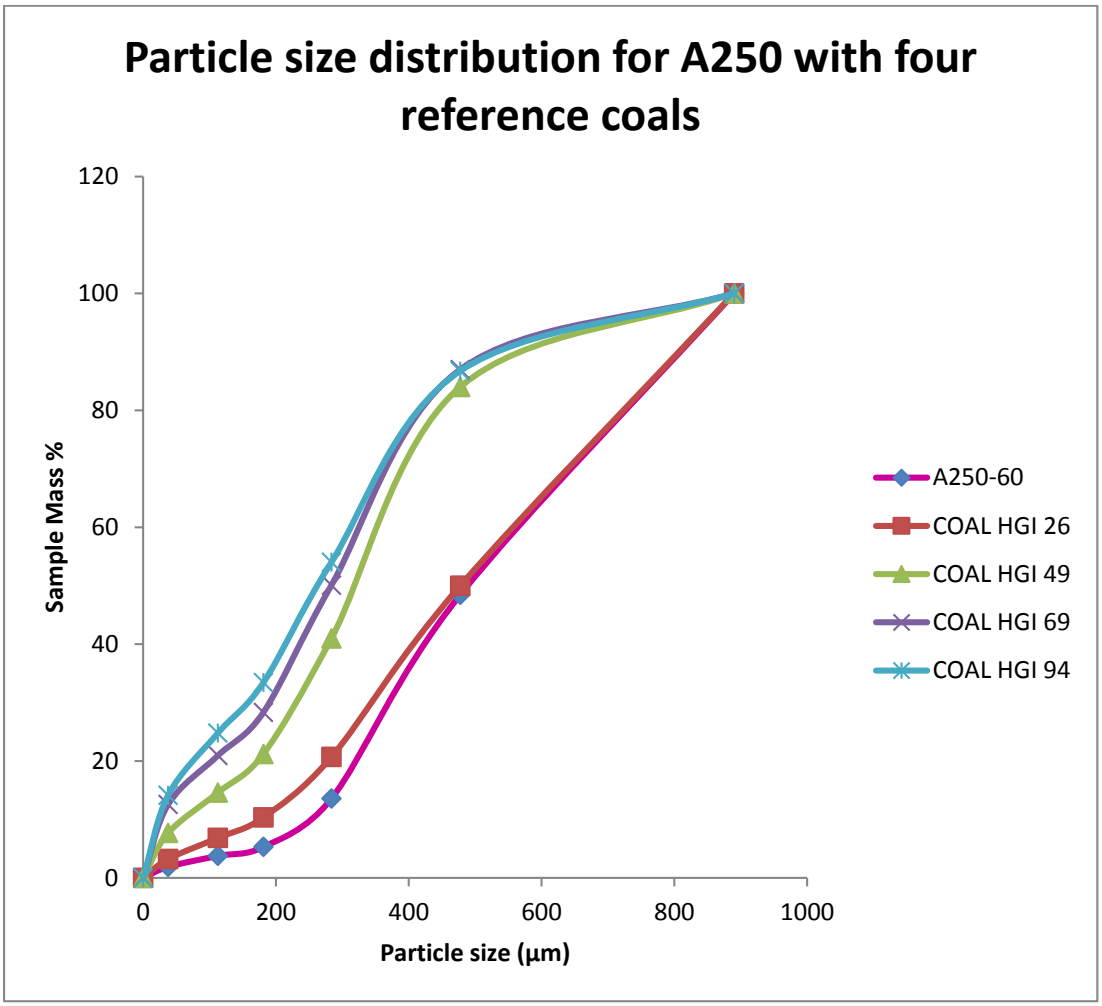

Figure 14. Particle size distribution for willow torrefied at 250°C for 60mins (A250-60) with four reference coals [66].

4.4 Equilibrium moisture content

The equilibrium moisture content (EMC) value is used as an indicator of hydrophobicity.

EMC was measured via static desiccators technique [38–39].The samples are exposed to a constant relative humidity (R_H) and temperature by placing desiccators containing the samples along with a saturated water/salt solutions into incubators set at ~ 30°C. Samples of untreated biomass and torrefied biomass at different temperatures were tested using a range of different R_H environments.

4.4.1 Experimental procedures

All samples were oven dried at 105 °C for 24 hours before being used in EMC tests. A biomass sample of about 0.5 g was weighed and placed into a Petri dish on a stand in a transparent chamber (Scienceware 420220000,Bel-Art) containing a selected salt solution. The plastic stand prevents direct contact between the solid samples and the saturated aqueous salt solution.

Desiccant and five different salt solutions were used to produce six relative humidities in a range from 0 to 94%. The equilibrium humidity of different saturated salt solutions are available in the literature from Greenspan [45]. The salt solutions were prepared by dissolving the salt crystals in deionized water at room temperature. Excess salt was added to saturate the solutions and to ensure constant relative humidity conditions [52]. A combination temperature and relative humidity monitor (HOBO UX100-011, Onset) was placed in each chamber to record the environment over the duration of each test.

The chambers were then placed in an incubator for temperature control. Tests in which samples were weighed daily showed that all samples reached equilibrium in four days. This required that each sample be removed from the chamber and exposed to ambient conditions. To

avoid this disruption in environmental conditions, the weight of the Petri dish and sample was measured and recorded only at the beginning and at the completion of the four day test. All tests were replicated three times and average values of EMC were calculated from the data.

4.4.2 Data analysis

The effect of torrefaction on hydrophobicity is determined by measuring how much moisture was absorbed by untreated and torrefied biomass and the associated rates of moisture weight gain.

The EMC determined from the experimental data was compared with the equilibrium moisture data predicted by the Modified Henderson Equation, modified Chung-Pfost Equation, modified Oswin Equation and VCSM equations. The VCSM model was expected to describe EMC accurately according to several literature sources [38,39].

Minitab software package was used for the statistical analysis. The least square method was applied to find the best model for each specific sample. The fitting of non-linear regression models including the best-fitting values for the equation constants and error parameters such as the standard error of estimate (S.E.) and the residual sum of squares (RSS). The best-fitting isotherm equation was predicted based on values of error parameters.

$$S.E. = \sqrt{\frac{(Y-Y')^2}{df}} \tag{17}$$

$$RSS = \sum (Y - Y')^2 \tag{18}$$

where Y and Y' are the measured and predicted values, respectively, and df is the degree of freedom.

For the analysis of VCSM model (see section 2.3), the nature of biomass helps determine initial estimates of the parameters. Bellur et al. (2009) suggest some useful guidelines. In this model, σ refers to the fraction of the adsorption capacity of biomass and it should be less than 1. The Flory-Huggins parameter χ, which determines compatibility of water and biomass, should be much greater than 0.5 because below this point, polymer and solvent are completely miscible. The energy parameter for adsorption, $\Delta\varepsilon$, should be close to the dimensionless heat of solidification of water in magnitude. The total EMC (ω), sum of the adsorbed (bonded) water (θ) plus the water in the non-adsorbed phase (non-bonded) (α) should be less than 1 (as a function of the total water in the system).

4.4.3 Preliminary test

Untreated Leucaena and torrefied Leucaena produced at temperatures of 210, 230, 250, and 270°Cwere used as 5 different samples for EMC determination. Desiccant (Fisher S161-500 Silica Gel), deionized water, and aqueous solutions saturated with K_2CO_3 , NH_4NO_3, NaCl, KCl, and KNO_3 and were used to maintain constant relative humidity environments based on ASTM method E104-02 (2012) [44].A constant experiment temperature of 32°C was maintained using an incubator.

Five samples were put inside each RH environment chamber and each sample started with an initial dry weight of 0.5g. The desiccant, NaCl, KCl, and KNO_3saturated aqueous solutions, and

deionized water produced relative humidity environments of 0, 75, 85, 94% and 100%, respectively.

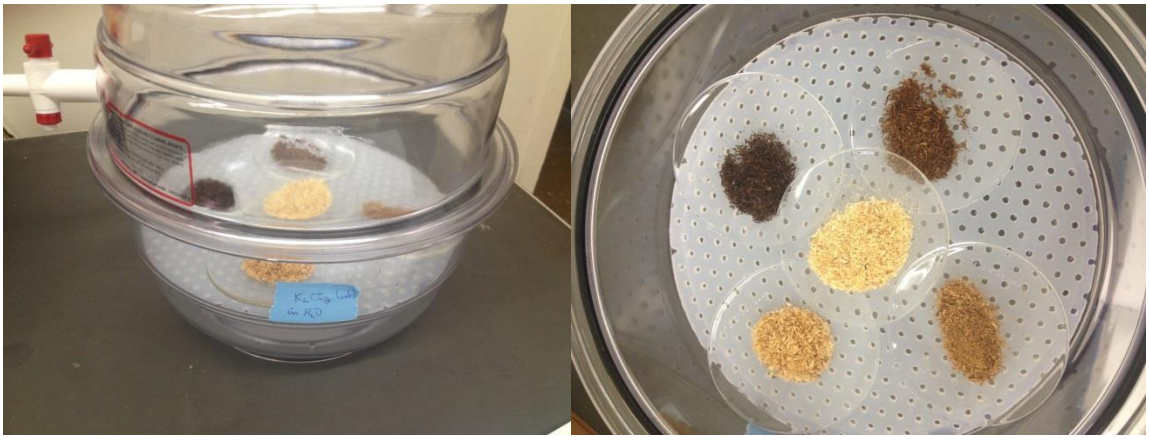

Figure 15. RH environment chambers and samples in EMC experiment.

The weight of each sample with holder was measured every 24 hours. A sample was assumed to be at equilibrium when three consecutive weight measurements showed a difference less than 1 mg.

Curves showing the sample weights versus time for preliminary tests are shown in Figure 16.

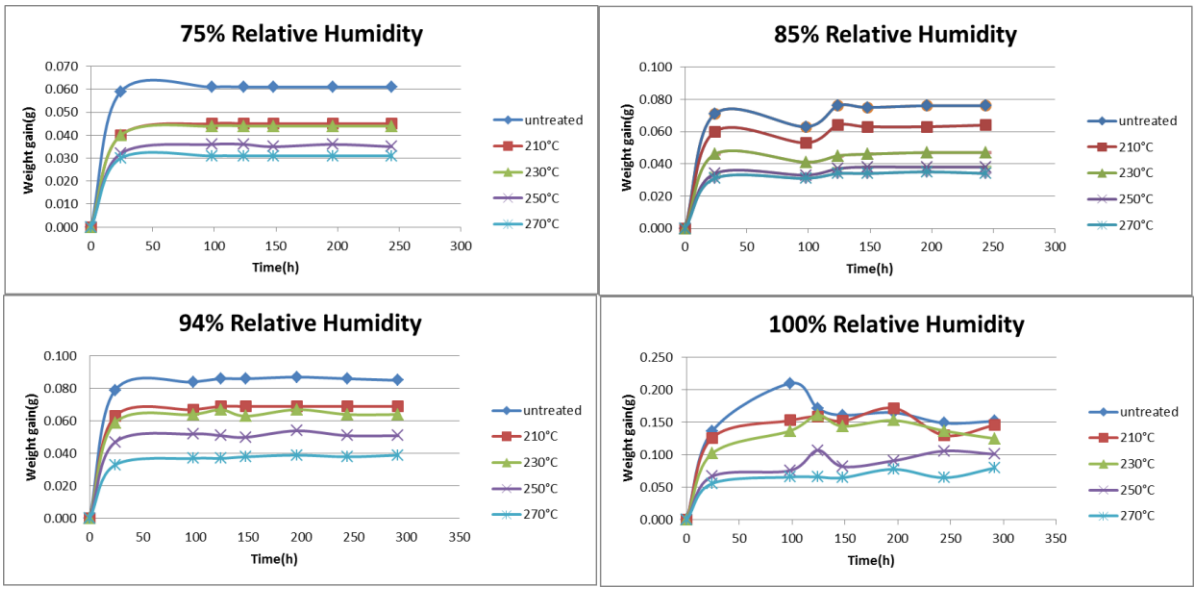

Figure 16. Leucaena weight gain versus time under four different relative humidity environments (a 75%, b 85%, c 94% and d 100%).

For a clear understanding, weight gain percentage verse relative humidity figure is also produced:

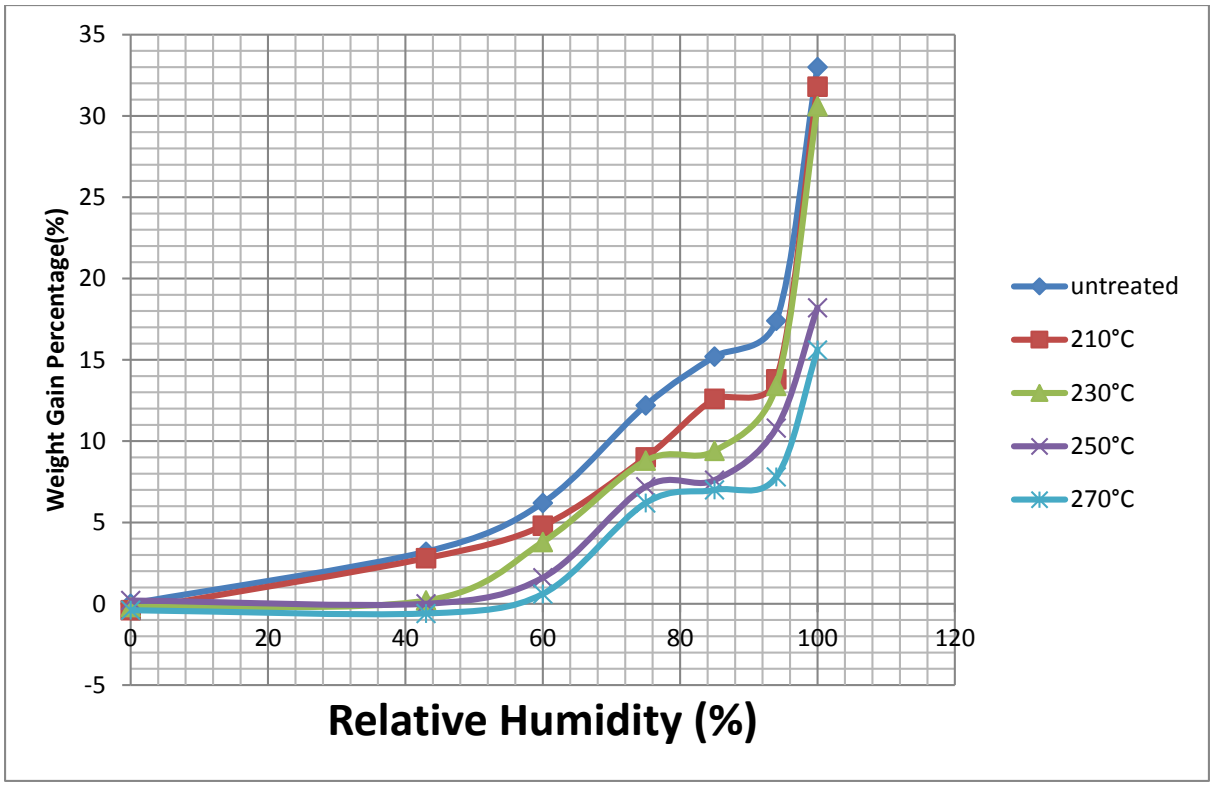

Figure 17. Leucaena weight gain percentage versus relative humidity.

- **5. Results and discussions**

This chapter describes the experimental results and presents analysis and discussion.

5.1 Fuel properties

The following sections discuss fuel properties of tested biomass species.

5.1.1 Mass yield, energy yield and HHV

Leucaena, energy cane, eucalyptus, sugarcane, sugarcane bagasse and banagrass were torrefied at muffle furnace controller setpoint temperatures of 220, 250, 270, 300, and 330°C, which resulted in corresponding average torrefaction temperatures measured in the fuel bed of 182, 206, 220, 248, and 273°C, respectively.

Table 7 – Torrefaction temperatures of different biomass materials under muffle furnace controller setpoint temperatures of 220, 250, 270, 300, and 330°C. UT = Untreated

T_{oven} [°C]	UT	220	250	270	300	330
Biomass material	$T_{torrefaction}$ [°C]					
Leucaena	25	183	211	225	253	279
Eucalyptus	25	187	206	225	244	269
Energy Cane S0	25	174	194	208	249	268
Energy Cane S3	25	185	204	217	250	273
Purple Bana S0	25	180	208	226	244	275
Purple Bana S3	25	188	206	225	251	274
Sugar Cane S0	25	182	214	226	248	278
Sugar Cane S3	25	178	206	214	251	272
Sugar Cane Bagasse	25	181	201	218	238	272
Average	25	182	206	220	248	273
STDV	0	4.4	5.7	6.5	4.7	3.7

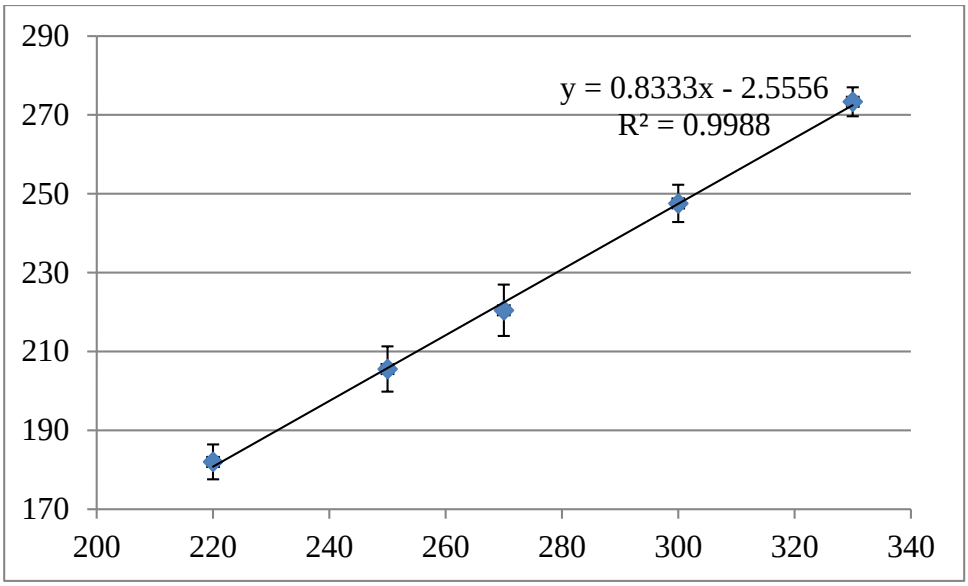

Figure 18. Correlation of muffle furnace controller setpoint temperatures and average torrefaction temperature.

For the energy cane, banagrass and sugar cane, one half of the harvested material was dried to ambient equilibrium moisture content after shredding (S0) and the other half was treated (S3) to reduce water soluble inorganic elements, principally K and Cl levels. For details please refer to section 4.1. The commercial sugarcane was harvested from experimental plots on the Hawaiian Commercial & Sugar Co. (HC&S) plantation at Puunene, HI. HC&S was also the source of sugar cane bagasse, the fibrous byproduct of sugar manufacturing in their Puunene factory.80g samples of torrefied material were generated at each torrefaction temperature. Initial and final weights and HHVs were measured for each test.

Table 8 shows the effects of torrefaction temperature on mass loss (mass yield), higher heating values, and energy yield. Energy yield is the ratio of chemical energy contained in the torrefied product to the chemical energy contained in the parent biomass. The mass loss and

higher heating value of all samples increased with torrefaction temperature, and the energy yield of the samples decreased accordingly. Between 200 and 300°C, dehydration and devolatilization of hemicellulose is presumed to be the main contributor to mass loss, and the severity of reaction increases with temperature [3].

Table 8 – Mass loss, HHV and energy yields of biomass species at tested torrefaction temperatures.

	T [°C]	mass loss [%]	HHV [MJ/kg]	Energy yield [%]
Leucaena	25*	0	19.2	100.0
	182	1.9	19.2	98.1
	206	3.5	19.3	97.0
	220	7.5	20	96.4
	248	14.5	20.8	92.6
	273	30	22	80.2
Eucalyptus	25*	0.0	18.9	100.0
	182	1.4	19.2	98.6
	206	2.1	19.5	99.4
	220	7.9	19.5	94.5
	248	15.2	20.1	88.8
	273	26.6	21.7	83.0
Energy Cane S0	25*	0	17.1	100.0
	182	11.2	18.9	95.9
	206	16.9	19.3	91.6
	220	20.4	19.8	90.1
	248	29.2	20.8	84.2
	273	39.5	22.8	78.8
Energy Cane S3	25*	0	18.5	100.0
	182	1.9	18.7	99.2
	206	4.3	19.1	98.8
	220	9.4	19.5	95.5
	248	22.1	20.7	87.2
	273	29.3	22	84.1
Purple Bana S0	25*	0	17.1	100.0
	182	4.8	17.6	98.0
	206	10.9	17.9	93.3
	220	16.2	18.6	91.2
	248	24.2	19	84.2
	273	38.1	20.6	74.6

* T= 25°C indicates biomass is untorrefied.

Table 9 – Mass loss, HHV and energy yields of biomass species at tested torrefaction temperatures (continued).

	T [°C]	mass loss [%]	HHV [MJ/kg]	Energy yield [%]
Purple Bana S3	25*	0	18.2	100.0
	182	2.2	18.7	100.0
	206	4.6	18.6	97.5
	220	10.3	18.9	93.2
	248	20.7	20.4	88.9
	273	33	21.7	79.9
Sugar Cane S0	25*	0	17.5	100.0
	182	11.8	19.2	96.8
	206	19.2	19.9	91.9
	220	25.7	21.5	91.3
	248	34.3	23.9	89.7
	273	45.7	25.6	79.4
Sugar Cane S3	25*	0.0	18.5	100.0
	182	2.6	19	100.0
	206	6.1	19.4	98.5
	220	10.1	19.8	96.2
	248	23.6	21.6	89.2
	273	29.3	22.7	82.9
Sugar Cane Bagasse	25*	0	17.9	100.0
	182	2.2	18.6	100.0
	206	4.9	18.5	98.3
	220	9.7	18.6	93.8
	248	18.8	19.6	88.9
	273	29.5	20.4	80.3

* T = 25°Cindicates biomass is untorrefied.

For better understanding of the data (Figure **19**), the nine biomass species are divided into four groups, and results for SCB (Sugar Cane Bagasse) are included in each group as a reference. Mass loss generally increases with temperature, presumably due mainly to hemicellulose

decomposition. Mass loss also becomes more severe as torrefaction temperature goes above 248°C, and this is related to depolymerization and decomposition of lignin and cellulose [23]. Based on Figure **19** a woody species, leucaena and eucalyptus, have similar mass loss trends and both lie below SCB, whereas other grassy S0 species all lie above SCB as shown in b, c and d. This indicates that woody species generally have smaller mass loss than untreated grassy species. Grassy S0species (EC-S0, PB-S0, SC-S0) are the uppermost curves in graph b, c and d, in the range of 5 – 45%. S3species values are closer to SCB and woody species, in a mass loss range of 2 – 35%, indicating that S3 treatment reduces the mass loss in torrefaction.

During torrefaction, biomass loses relatively more oxygen and hydrogen compared to carbon [3], [34], [38]. Consequently, the calorific value of the product increases as shown in Figure 19. Higher heating values of torrefied woody biomass and grass species (S0, S3) are in the range of 19 – 22MJ/kg and 17.5 – 26MJ/kg, respectively.

Trends of energy yield of the torrefied product materials as a function of torrefaction temperature are shown in Figure **21**. All nine species of biomass have an energy yield greater than 95% at 182°C. When torrefaction temperature increases, the energy yield decreases. Energy yield is substantially higher for woody and dewatered/leached (S3) grassy biomass compared to unwashed (S0) grassy species.

Energy yield of leucaena, eucalyptus and SCB presented in Figure **21** a ranges from 100% to 97.5%, for temperatures from 25 to 206°C, then decreases to ~95% at 220°C, and is further reduced to ~80% at 273°C.S3 species in Figure 20 b, c and d exhibit similar trends as SCB.

S0 energy yields are generally lower and display a much more rapid decrease as a function of torrefaction temperature. For instance, woody and S3 biomass maintain energy yields of ≥95% for torrefaction temperatures of ~210 – 220 °C. Energy yields of torrefied S0 biomass, however,

fall below 95% at temperatures ranging from185 – 200°C, and are ≤80% in a temperature range from 260 – 273 °C.

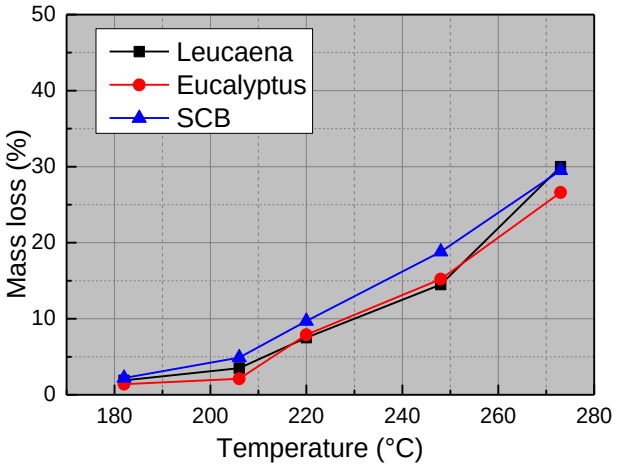

a

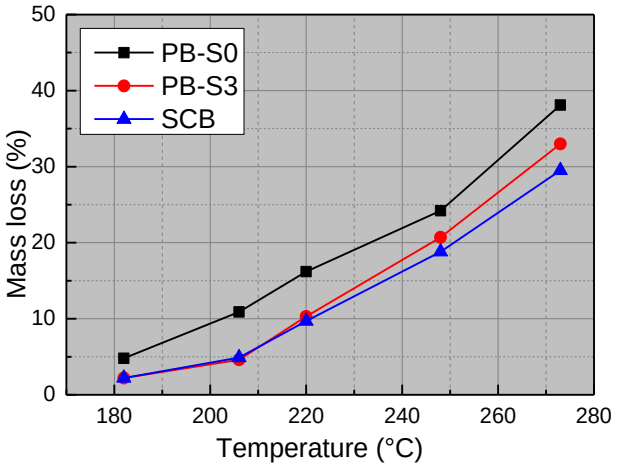

b

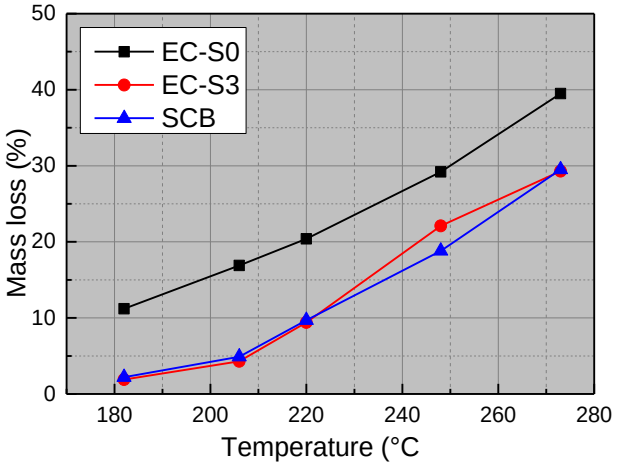

c

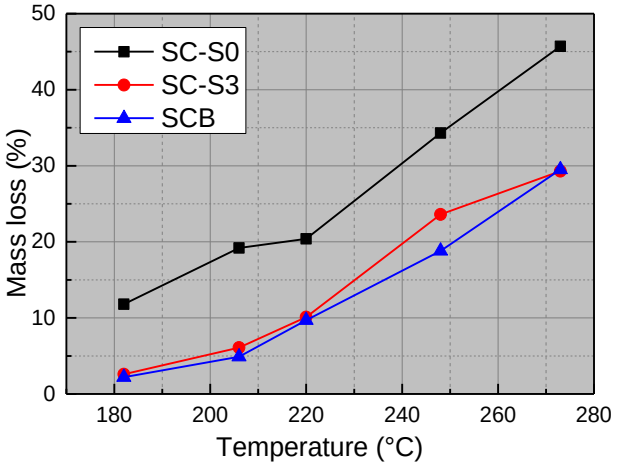

d

Figure 19. Effect of temperature on mass loss. Untorrefied parent materials have mass loss of zero.

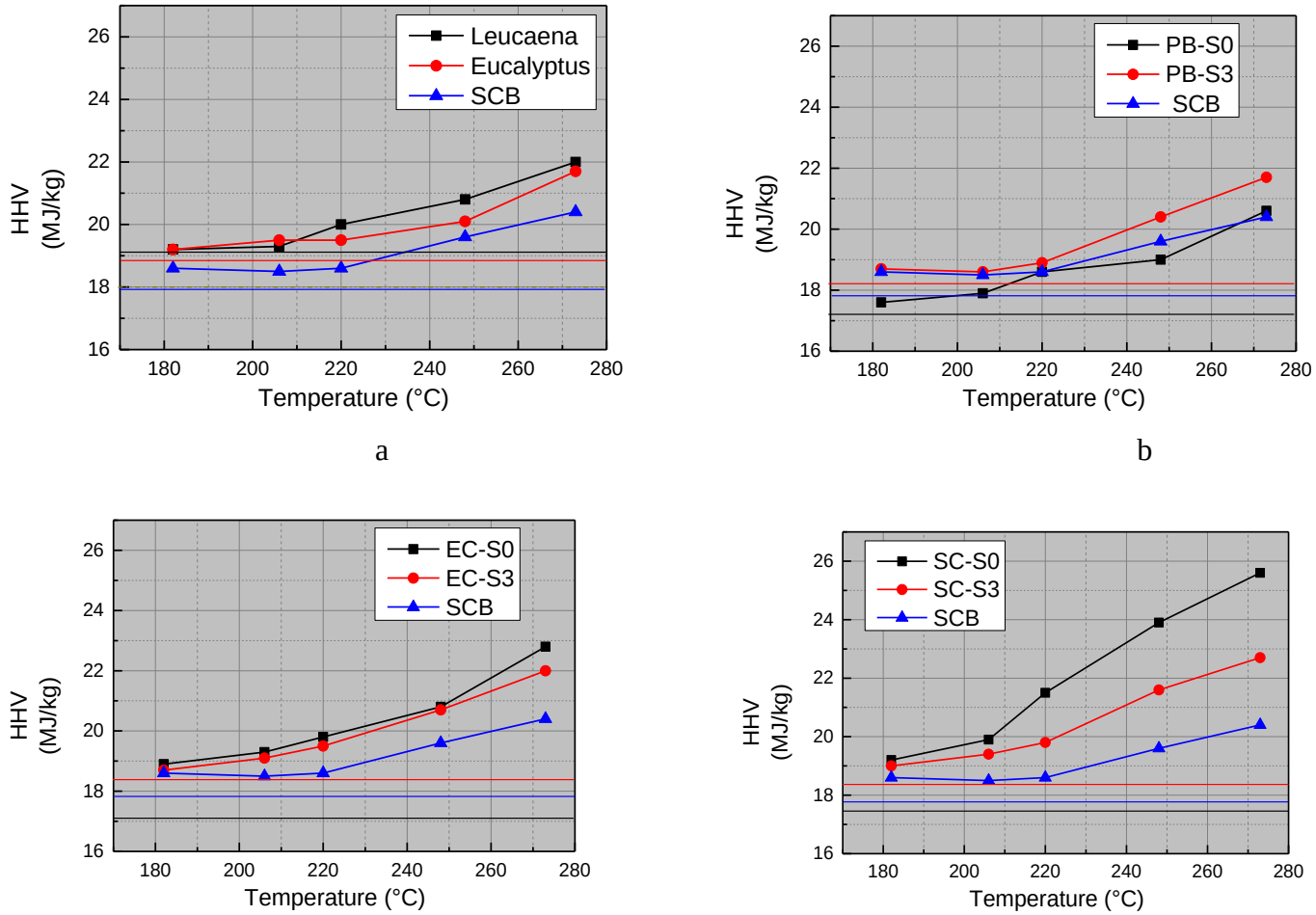

Figure 20. Effect of temperature on higher heating value. Lines indicated HHV of corresponding-colored, untorrefied, parent materials.

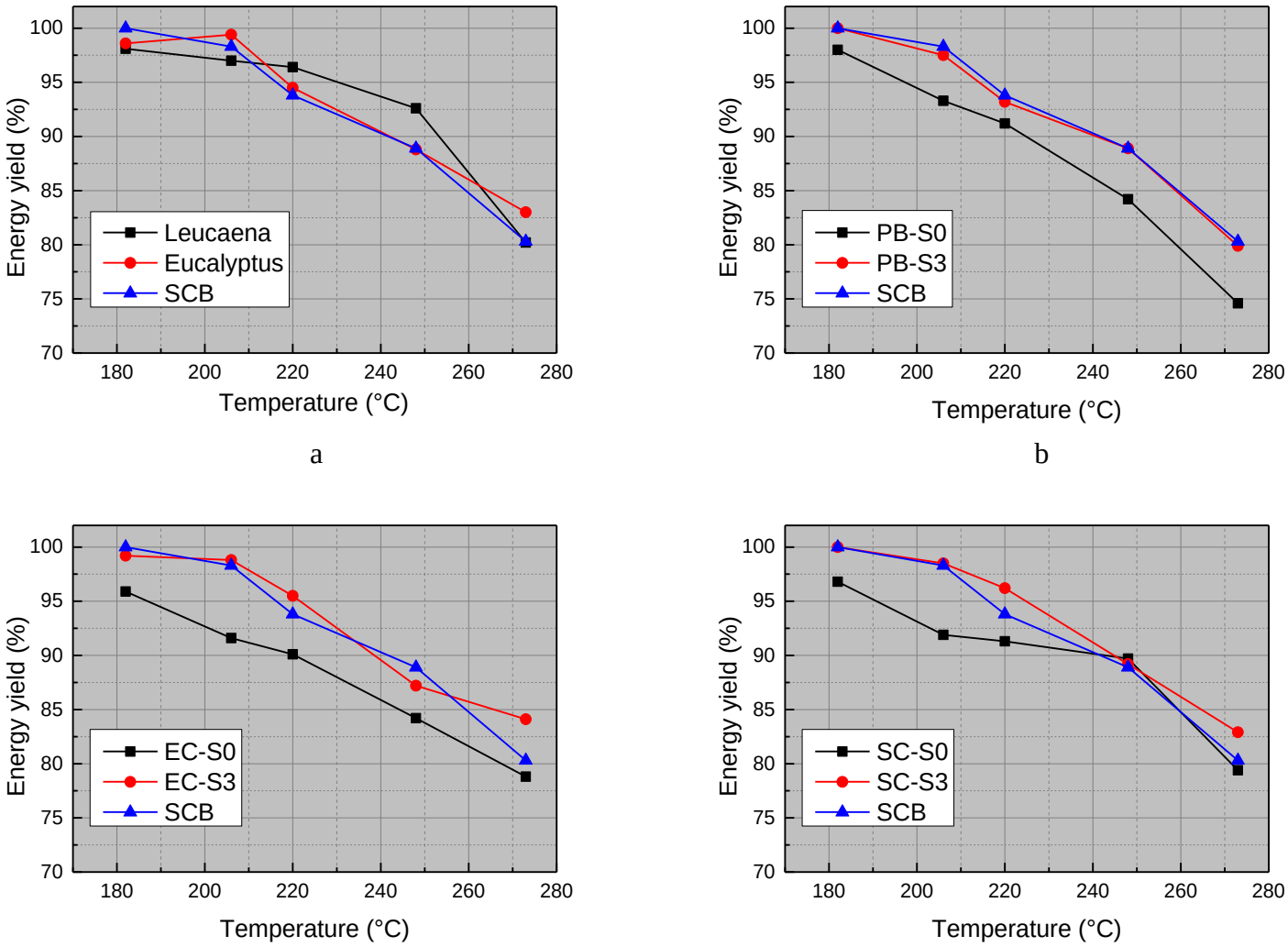

Figure 21. Effect of temperature on torrefaction energy yield, biomass pre torrefaction treatment has energy yield =100%.

5.1.2 Ultimate and proximate analysis

Ultimate and proximate analyses were completed for all nine biomass materials at six torrefaction temperatures. Ultimate analysis was conducted in the SOEST Laboratory for Analytical Biogeochemistry, University of Hawaii at Manoa, with a CE-440 Elemental Analyzer. All samples were ground to ≤75μm to assure uniformity. Results from testing untorrefied eucalyptus and eucalyptus torrefied at 220°C and 248°C had standard deviations <1% (relative), indicating excellent repeatability. Proximate analyses were conducted by Hazen Research, Inc. Preparation of samples was carried out in accordance with ASTM Standard D3172-13 [62].Ultimate and proximate analysis data of all torrefied biomass species versus torrefaction temperatures are presented in Table 10:

Table 10 – Proximate and ultimate analysis data on dry basis (unit: wt %), 25°C= untorrefied.

Leucaena	Ash	Volatile	Fixed C	C	H	N	O (residue)
25° C	0.86	84.28	14.86	50.12	4.97	0.38	44.53
182° C	1.03	84.41	14.55	50.96	5.16	0.66	43.22
206° C	1.65	83.71	14.64	51.25	5.13	0.55	43.07
220° C	1.64	80.21	18.15	52.65	5.23	0.53	41.59
248° C	1.90	75.33	22.78	53.25	5.18	0.50	41.07
273° C	1.86	70.50	27.64	57.19	5.01	0.59	37.21
Eucalyptus	Ash	Volatile	Fixed C	C	H	N	O (residue)
25° C	0.74	87.40	11.86	48.83	4.94	0.20	46.03
182° C	0.57	87.48	11.94	50.28	4.84	0.22	44.66
206° C	0.65	87.79	11.57	50.71	5.04	0.28	43.97
220° C	0.54	86.70	12.75	50.84	4.84	0.25	44.07
248° C	0.65	81.63	17.72	52.65	4.98	0.24	42.12
273° C	0.70	75.26	24.05	55.81	4.87	0.18	39.14

EC-S0	Ash	Volatile	Fixed C	C	H	N	O (residue)
25° C	5.58	79.54	14.88	46.81	4.74	0.49	47.97
182° C	7.03	74.58	18.39	47.81	4.82	0.57	46.80
206° C	7.83	72.33	19.84	50.22	4.80	0.56	44.42
220° C	7.73	71.15	21.12	50.24	4.78	0.60	44.38
248° C	8.38	65.40	26.22	53.22	4.50	0.66	41.62
273° C	10.05	59.08	30.86	55.38	4.25	0.70	39.67
EC-S3	Ash	Volatile	Fixed C	C	H	N	O (residue)
25° C	2.89	89.81	7.30	47.86	5.08	0.40	46.66
182° C	2.80	87.21	9.98	49.45	5.23	0.54	44.79
206° C	3.10	86.58	10.32	48.95	5.19	0.52	45.34
220° C	3.75	83.85	12.40	49.92	5.24	0.48	44.37
248° C	3.74	77.25	19.01	52.26	5.12	0.42	42.20
273° C	4.06	78.33	17.61	54.64	4.97	0.46	39.93

PB-S0	Ash	Volatile	Fixed C	C	H	N	O (residue)
25° C	8.47	79.63	11.90	51.67	4.71	0.59	43.03
182° C	7.99	77.41	14.61	51.53	4.71	0.62	43.14
206° C	9.41	73.60	16.99	50.30	4.99	0.63	44.08
220° C	6.71	74.82	18.47	51.19	5.04	0.55	43.21
248° C	11.84	63.84	24.32	53.35	4.90	0.48	41.27
273° C	13.11	59.41	27.48	56.55	4.72	0.46	38.27
PB-S3	Ash	Volatile	Fixed C	C	H	N	O (residue)
25° C	4.69	81.60	13.71	49.23	5.11	0.32	45.34
182° C	5.61	82.75	11.64	49.30	5.14	0.36	45.21
206° C	5.26	83.19	11.55	49.18	5.05	0.41	45.36
220° C	4.78	79.40	15.82	49.81	5.03	0.42	44.74
248° C	6.84	73.94	19.22	52.93	5.04	0.42	41.62
273° C	8.17	66.10	25.72	55.78	4.77	0.49	38.95

Table 10 – Proximate and ultimate analysis data on dry basis (unit: wt %), 25°C= untorrefied. (Continued).

SC-S0	Ash	Volatile	Fixed C	C	H	N	O (residue)
25° C	2.52	83.01	14.46	47.61	4.47	0.39	47.52
182° C	3.27	76.48	20.25	51.03	4.63	0.44	43.90
206° C	2.92	72.93	24.15	53.81	4.63	0.46	41.10
220° C	3.57	68.71	27.72	54.83	4.57	0.48	40.12
248° C	3.48	62.20	34.32	57.76	4.30	0.48	37.46
273° C	4.68	49.81	45.51	64.96	3.72	0.55	30.76
SC-S3	Ash	Volatile	Fixed C	C	H	N	O (residue)
25° C	2.06	87.81	10.14	48.94	4.92	0.30	45.83
182° C	2.16	87.29	10.55	49.85	5.12	0.33	44.69
206° C	2.08	87.67	10.25	50.40	5.16	0.34	44.10
220° C	1.71	85.16	13.13	50.81	5.24	0.33	43.62
248° C	2.46	81.05	16.49	53.21	5.11	0.38	41.30
273° C	3.07	73.90	23.03	56.45	4.73	0.40	38.42
SCB	Ash	Volatile	Fixed C	C	H	N	O (residue)
25° C	7.74	79.99	12.28	47.51	5.07	0.45	46.96
182° C	5.11	81.83	13.06	47.34	5.07	0.46	47.13
206° C	6.62	81.27	12.11	47.24	4.97	0.39	47.41
220° C	7.96	78.51	13.54	48.05	5.02	0.37	46.56
248° C	6.85	76.40	16.75	50.97	5.01	0.38	43.64
273° C	12.53	67.58	19.89	53.33	4.72	0.39	41.56

Carbon content of the highest-temperature torrefied materials increased by 5 to 8.5% (absolute) compared to the untorrefied parent materials with the exception of SC-S0 which increased 17%. O decreased correspondingly, from 5 to 8% (absolute) with the same behavior by SC-S0 which decreased 17% (absolute). H content varied slightly over the range of torrefaction temperatures but did not display a clear trend. The greater change in C and O content for the SC-S0 samples can be attributed to the presence of sugars which are more labile than the cellulose and hemicellulose components of fiber. Nitrogen contents ranged from 0.18 to 0.7% across all

samples but did not show a clear trend or dependence on torrefaction temperature. In all cases, the greatest changes occur at torrefaction temperatures ≥248 °C.

The proximate analysis yielded results for fixed carbon, volatile matter, and ash. Fixed carbon content of the material torrefied at the highest temperature are generally increased by 12 and 15% (absolute) compared to the parent materials and are comparable across the materials with two exceptions. SCB and SC-S0 present extremes in fixed carbon changes of 7.5% and 31% (absolute), respectively. Increases in fixed carbon content are offset by decreases in volatile matter. While the overall mass loss results in reduced elemental mass for C, H, and O, ultimate and proximate analyses highlight increases in carbon (total and fixed) concentration and decreases in volatile matter/O concentration, with roughly constant H concentration, resulting in increased heating values and energy-denser materials [13~14], [27~28], [30].

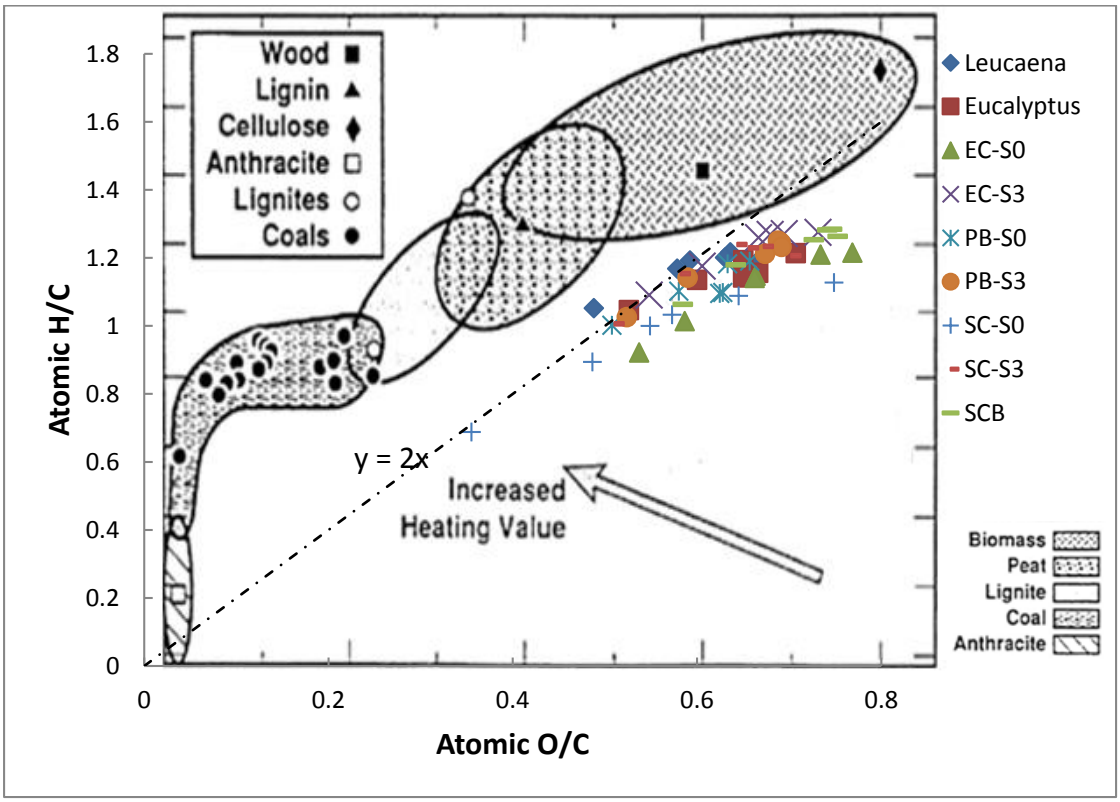

Figure 22.Van Krevelen diagram for tested biomass, coals, and several known species [34], [67].

Elemental composition of biomass can be an indicator of feedstock quality as illustrated by the Van Krevelen diagram shown in Figure 21. The H/C= 2 O/C trend line in the diagram represents the dehydration reaction pathway. As the severity of torrefaction increases, the biomass dehydrates, moving from the upper right in the diagram toward the lower left and shifting toward properties displayed by coals. As seen in the tabulated data, the largest changes in element ratios occur at the upper end of the torrefaction temperature range. This diagram also shows that among all nine types of biomass tested, sugar cane (SC-S0) had the greatest alteration in element ratios, which is expected due to its high carbon increase through torrefaction.

5.2 Grindability

Standard reference coal materials with known HGI values of 27, 47, 64, and 89 were obtained from the Australian Coal Preparation Society's (ACPS) CHOICE Analytical Pty Ltd. Calibration of the 500 mL ball mill was performed**.** Figure 23 shows the plot of the amount of sample that passed through a 75 μm sieve against the HGI values of the four coals. The figure indicates that coals with higher HGI are easier to grind. A calibration curve was generated from those standard coals of known HGI values as shown in Eq. 18.

$$y = 1.6999x + 14.64 \quad (19)$$

Where:

y = HGI value

x = percentage of sample smaller than 75 micron

Eq. 18 was then used to determine the equivalent HGI of the nine biomass materials.

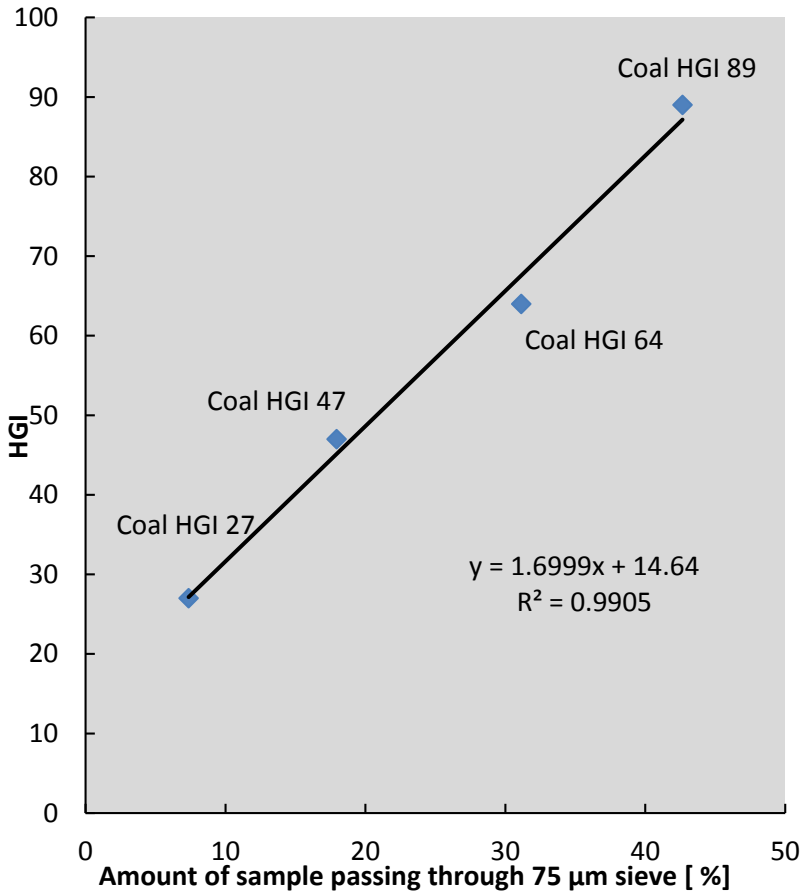

Figure 23. Curve relating HGI of standard reference material coals with the percentage sample mass passing through a 75 µm screen after ball milling.

During the torrefaction process, the decomposition of hemicellulose weakens the viscous and elastic characteristics of woody cell wall, and the depolymerization of cellulose and thermal softening of lignin may also contribute to weakening the cell wall in vegetative material [8, 16, 33]. Figure 24 illustratesHGI values of all nine species in relation to torrefaction temperature during torrefaction. In line with earlier studies, grindability of biomass improves with increasing torrefaction temperature. For untorrefied biomass, HGI values fall between 18 and 21, and are much lower than HGI values of most coals, indicating that biomass pre- torrefaction treatment

requires more grinding energy than coals. Comparing biomass at the highest torrefaction temperature to untorrefied biomass shows that the HGI value increased 2 – 4.5 times, falling in range from 54 to 107. Leucaena represents the lower end of the range, while energy cane S0 is the highest.

At the two lower torrefaction temperatures, the HGI values of all the samples showed minor improvements, with maximum HGI values of 32, less than double than that of the initial, untorrefied materials. With torrefaction temperatures ≥220 °C, the rate of improvement in HGI is more dramatic. With the exception of leucaena, torrefaction temperatures ≥248 °C result in a doubling of the HGI values compared to the untreated samples.

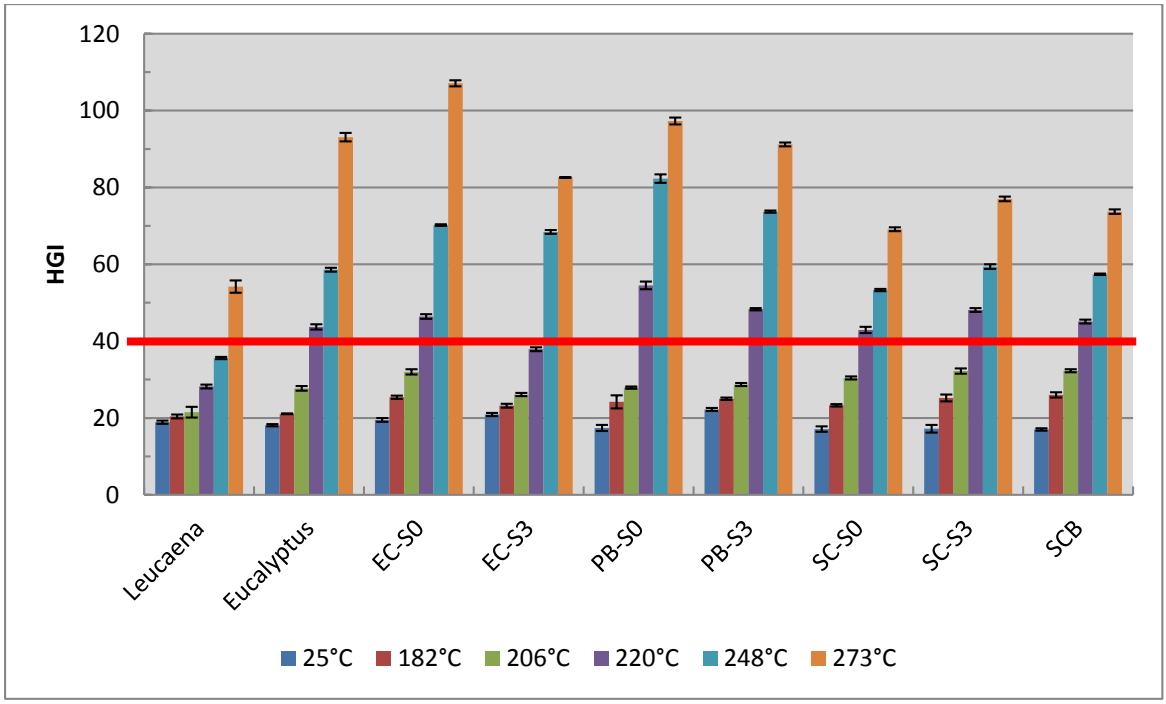

Figure 24. Hardgrove Grindability Index (HGI) of tested species in relation to torrefaction temperature during torrefaction. Red line represents HGI of 40. Torrefaction temperature of 25°C is untorrefied parent material.

For practical context, coal from the local AES Hawaii Power Plant (Kapolei, Hawaii) was sampled and analyzed using the identical technique. Results determined an HGI value of 40 for the AES coal and this is shown in Figure 22 as a red horizontal line. Using an HGI of 40 as a benchmark, the effective minimum torrefaction temperature for each biomass material was calculated using linear interpolation and the results are listed in Table 11. With the exception of leucaena, an average effective torrefaction temperature of approximately 200-225°C is sufficient to improve grindability of the tested biomass to the level of coal from the AES Hawaii power plant. Leucaena requires a higher torrefaction temperature of ~ 260°C. Substantial differences were not in evidence between the treated fuels (S0 and S3) for banagrass, sugarcane, or energy cane.

Table 11 – Minimum effective torrefaction temperature to achieve HGI=40.

	Leuc	Euc	EC-S0	EC-S3	PB-S0	PB-S3	SC-S0	SC-S3	SCB
Min. temp. for HGI=40 [°C]	259	220	202	219	216	218	223	210	211

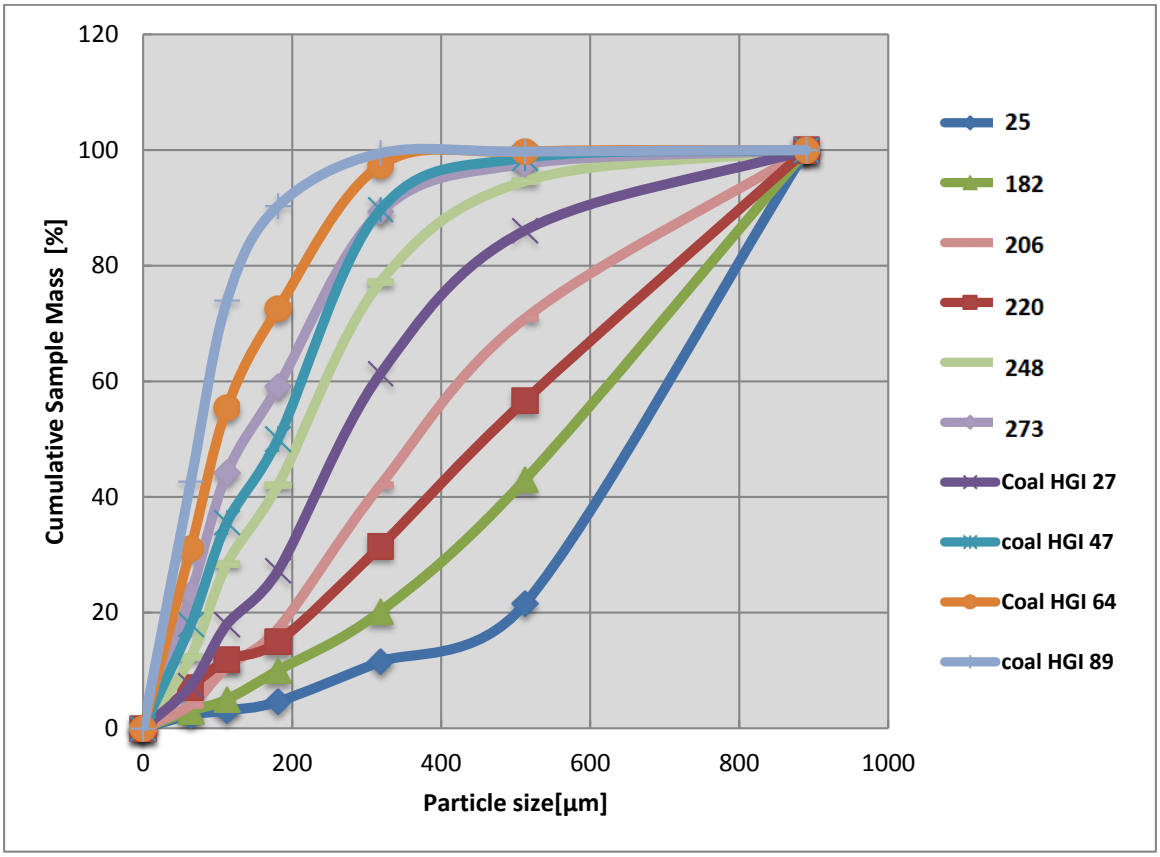

Figure 25. Cumulative particle size distributions of leucaena under different torrefaction temperatures and four reference coals resulting from grindability tests.

Figure 25 shows an example of the particle size distribution of a raw biomass sample (leucaena) and its torrefied counterparts after milling. The particle size distribution curves of the four reference coals are also shown for comparison purposes. With increasingly more severe torrefaction conditions, distinct improvement can be observed in grindability behavior of the leucaena samples. Particle size distributions curves of the torrefied biomass become increasingly similar to the reference coal curves, e.g. leucaena torrefied at a temperature of 273°C shows a comparable particle size distribution to coal with a HGI value of 47 under identical milling conditions. Similar trends were also observed in the other samples.

5.3 Equilibrium moisture content

Equilibrium moisture content tests were finished in triplicates for all untorrefied and torrefied biomass materials at 32°C. Equilibrium moisture content of biomass samples (wet basis) over a range of relative humidity from 0 – 94% are shown in Figures 24 to 32.

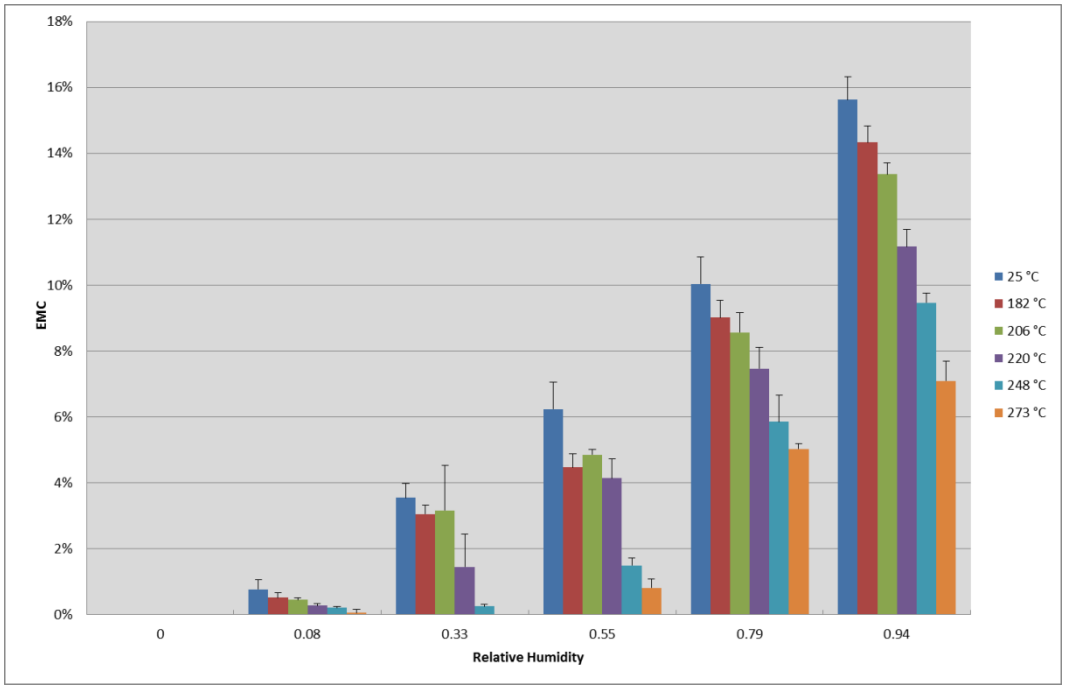

Figure 26. Summary of equilibrium moisture content test results for leucaena across a range of torrefaction temperatures.

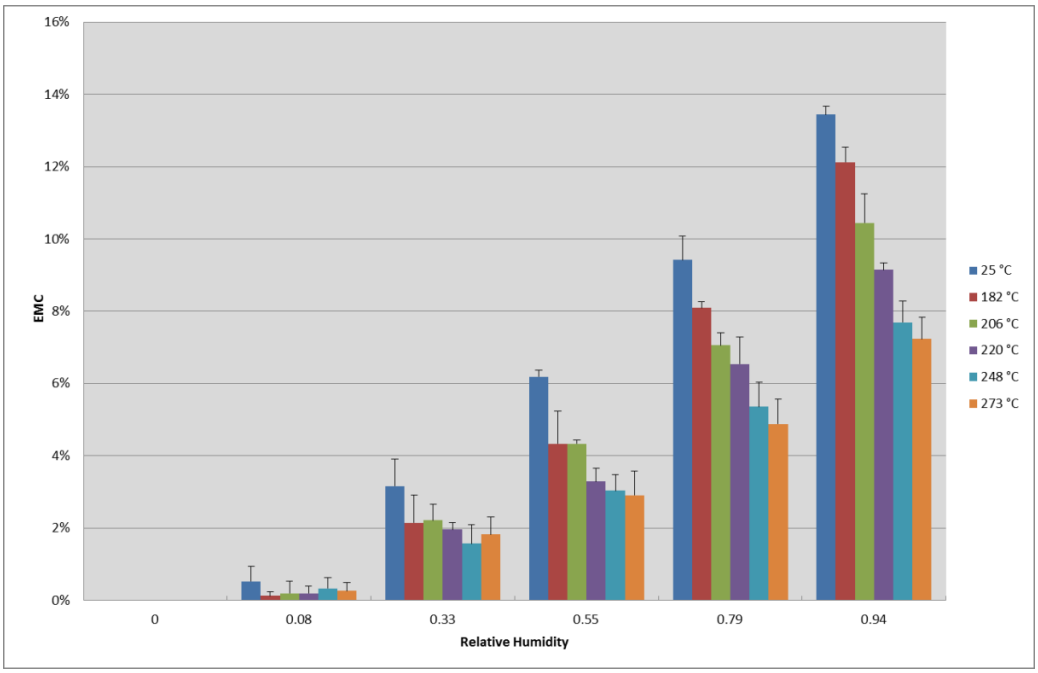

Figure 27. Summary of equilibrium moisture content test results for eucalyptus across a range of torrefaction temperatures.

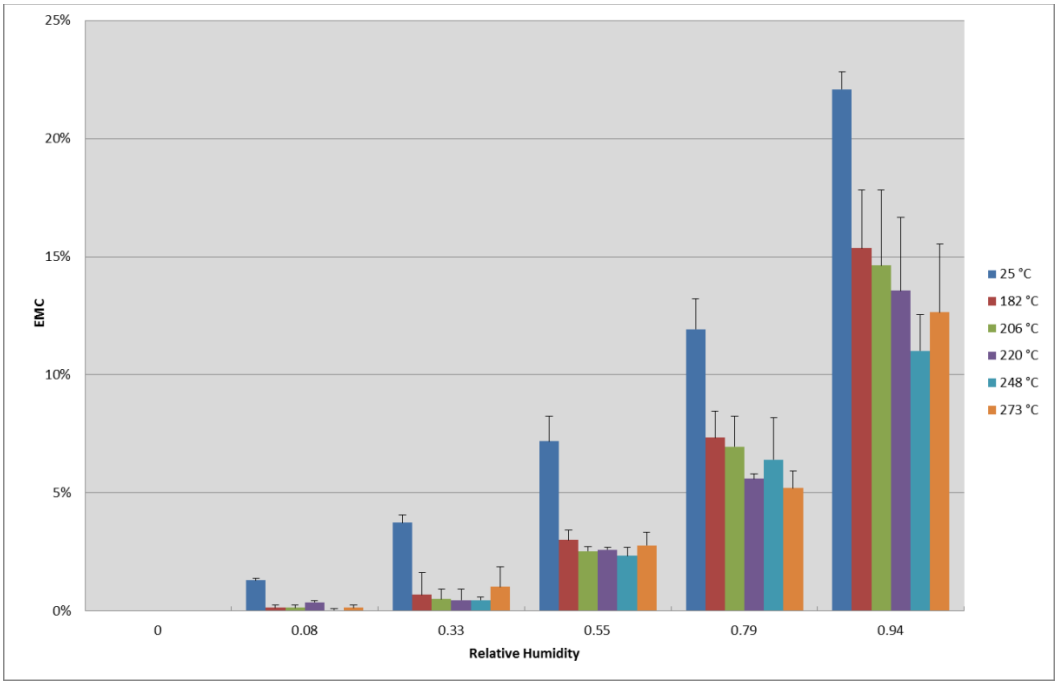

Figure 28. Summary of equilibrium moisture content test results for energy cane S0 across a range of torrefaction temperatures.

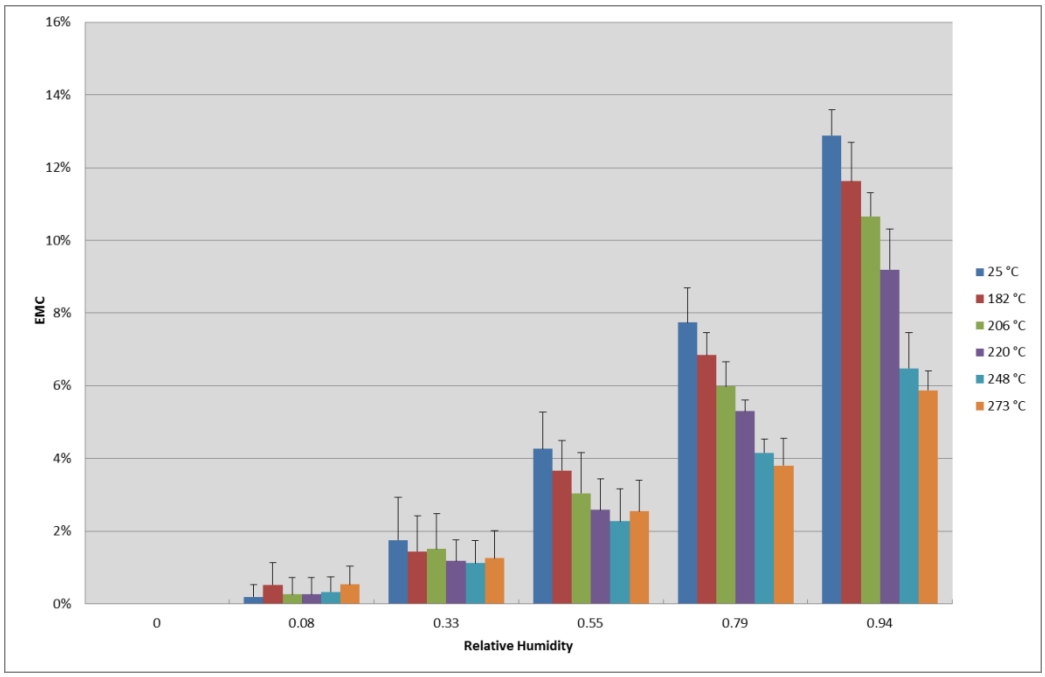

Figure 29. Summary of equilibrium moisture content test results for energy cane S3 across a range of torrefaction temperatures.

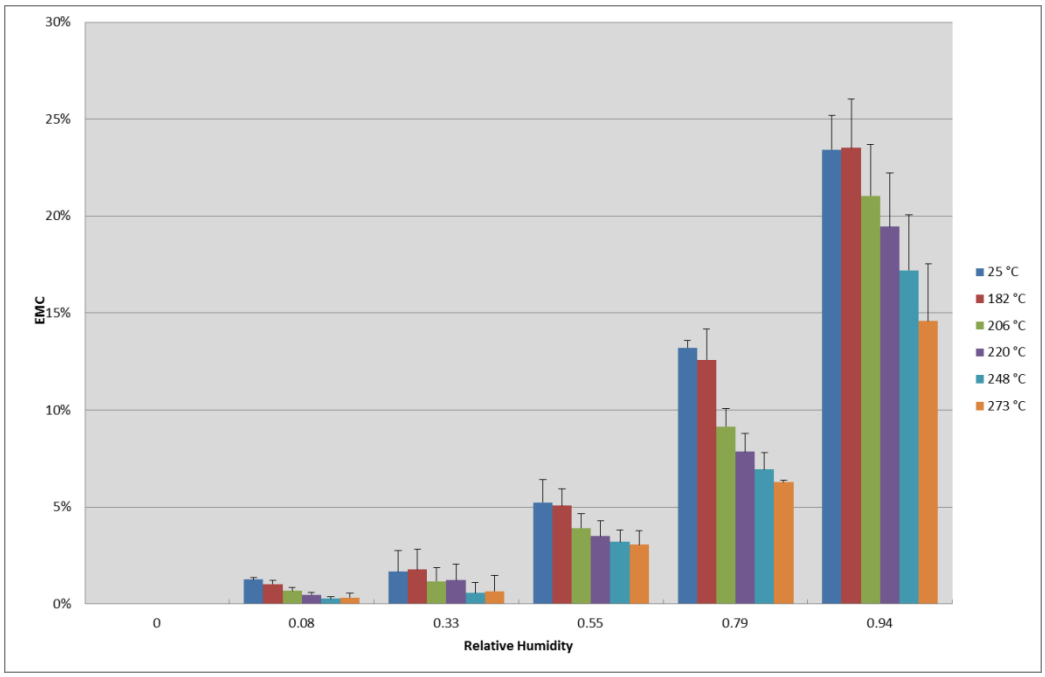

Figure 30. Summary of equilibrium moisture content test results for P-bana S0 across a range of torrefaction temperatures.

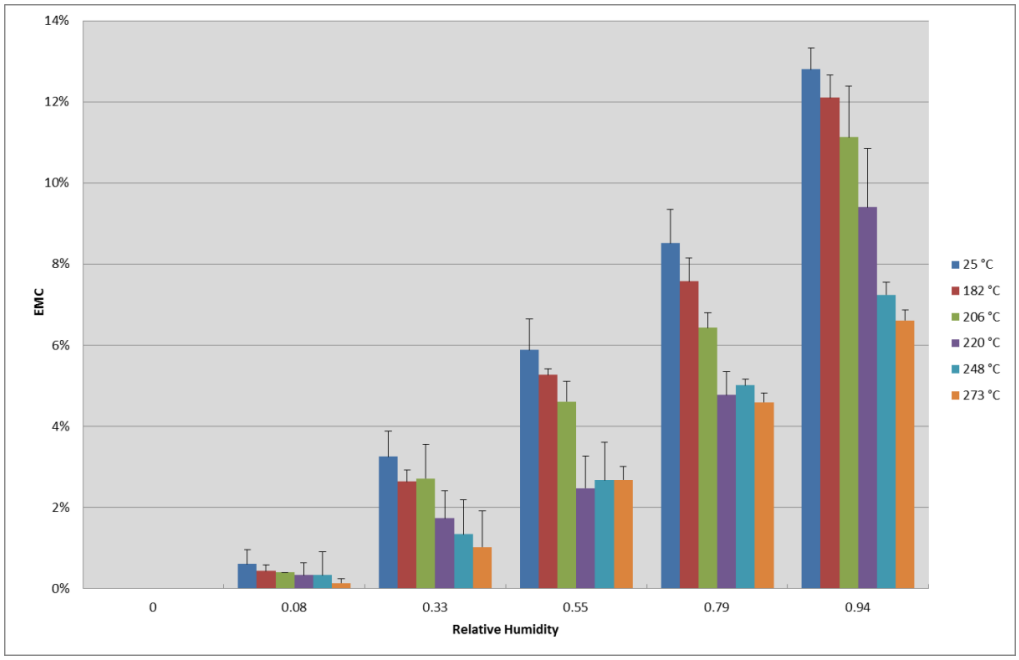

Figure 31. Summary of equilibrium moisture content test results for P-bana S3 across a range of torrefaction temperatures.

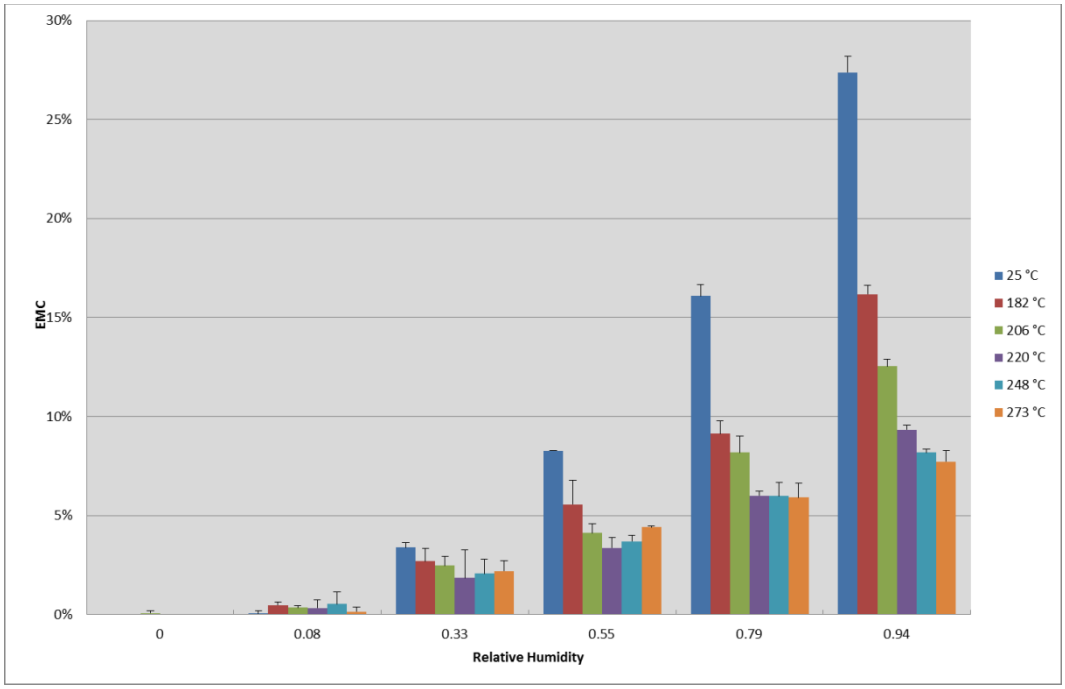

Figure 32. Summary of equilibrium moisture content test results for Sugarcane S0 across a range of torrefaction temperatures.

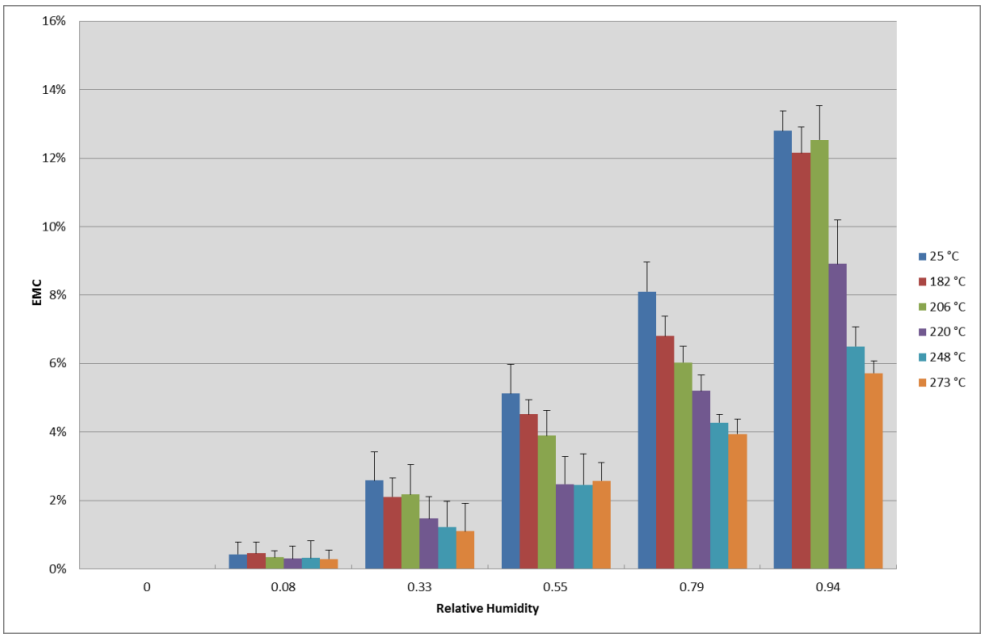

Figure 33.Summary of equilibrium moisture content test results for sugarcane S3 across a range of torrefaction temperatures.

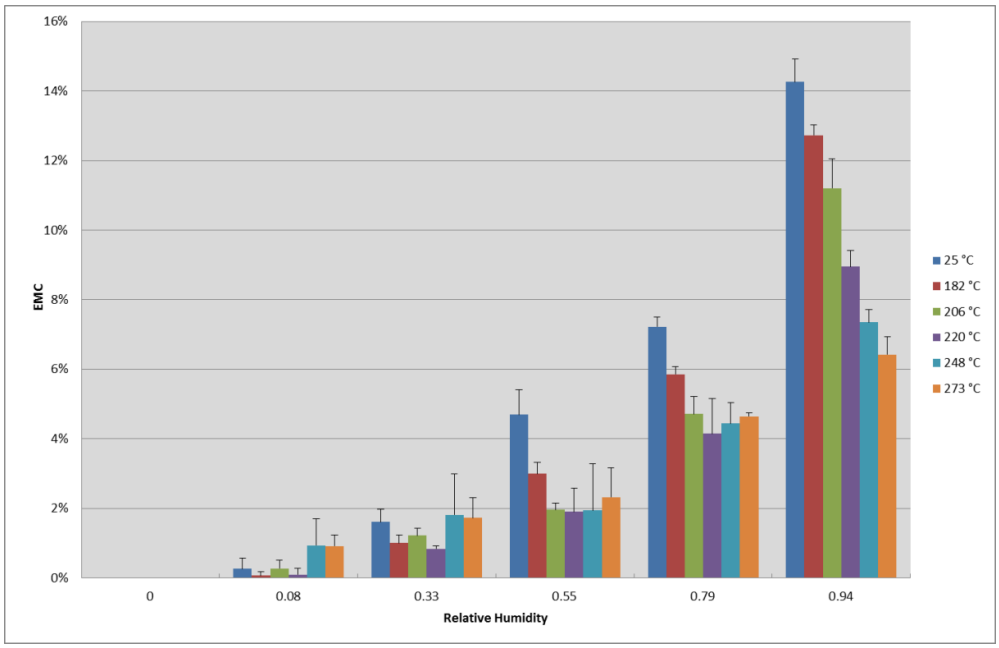

Figure 34. Summary of equilibrium moisture content test results for sugarcane bagasse across a range of torrefaction temperatures.

Table 12 – Summary of torrefaction temperatures (°C) required to produce a significant difference in hydrophobicity between the parent and torrefied materials at each relative humidity shown in Figures 24 to 32.

	Relative Humidity (%)					
Test Material	0	8	33	55	79	94
Leucaena	na*	248	220	182	206	182
Eucalyptus	na	na	220	182	182	182
Energy cane S0	na	182	182	182	182	182
Energy cane S3	na	na	na	na	206	206
P-bana S0	na	206	na	248	206	248
P-bana S3	na	na	220	220	206	220
Sugarcane S0	na	na	206	182	182	182
Sugarcane S3	na	na	na	220	206	220
Sugarcane bagasse	na	na	na	182	182	182

*na indicates no torrefaction temperature successfully increased hydrophobicity.

The figures show that the EMC of the biomass materials all increase with increasing relative humidity across the test range from 8% to 94%. Table 12 summarizes test results by identifying the minimum torrefaction temperature required at each relative humidity to produce a significant different between the EMC of the parent and torrefied materials. At relative humidity values of 0, 8, and 33%, little difference is apparent between the EMC's of the torrefied materials regardless of torrefaction temperature. At relative humidity ≥55%, the minimum torrefaction temperatures required to produce a significant difference (no error bar overlap) in EMC value generally ranged from 182 to 220°C, with two cases requiring 248°C. No consistent trend was found relating pretreatment for ash reduction with minimum temperature to affect hydrophobicity.

Comparing S0 to S3 species, EMC of S0 is generally higher than corresponding EMC for S3, e.g.at 94% relative humidity, EMC of untreated energy cane S0is 22.1±0.7%, whereas untreated

energy cane S3 is only 12.9±0.7%.Similarly at the highest torrefaction temperature, the S0 and S3 EMCs for energy cane were 12.7±2.9% and 5.9±0.5%. EMCs of untorrefied leucaena (EMC = 15.6±0.7%) and eucalyptus (EMC = 13.4±0.2%) and leucaena (EMC = 7.1±0.6%) and eucalyptus (EMC = 7.2±0.6%) torrefied at 273°C, show similar behavior to energy cane S3, sugarcane S3, P-bana S3, and sugarcane bagasse materials. This indicates that the dewatered leached grass species have similar hydrophobicity characteristics as wood materials both before and after torrefaction.

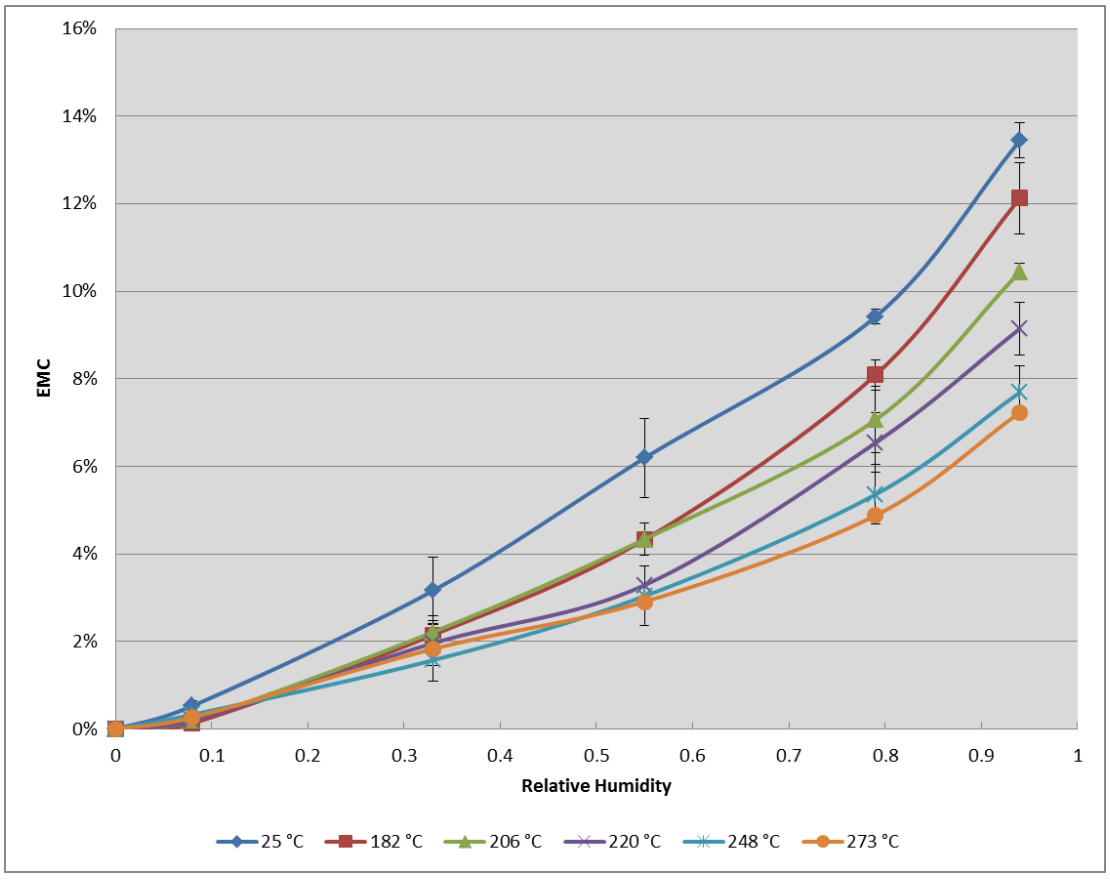

Figure 35. Summary of the dependence of EMC on relative humidity in untreated and torrefied eucalyptus.

Most biological products exhibit a characteristic sigmoidal isotherm [52], with a rapid increase in EMC at RH ≤~10%, followed by a moderate increase in EMC from 10 to 60% RH, and then a rapid increase in EMC at higher RH values. Figure 35 shows comparable data for eucalyptus and torrefied eucalyptus. The number of data points in the lower RH region <10% are not sufficient to clearly define the lower end of the sigmoidal curve, however the moderate increase at mid-range RH and rapid increase at high RH are readily apparent.

As discussed in section 2.3, the EMC of the biomass is the sum of the bonded water (θ) plus non-bonded water (α).

$$EMC = \alpha + \theta \tag{20}$$

At equilibrium:

$$\theta(\alpha+\theta)exp(\Delta\varepsilon) = \alpha(\sigma-\theta)exp(\Delta F) \tag{21}$$

$$(\alpha+\theta)HR = \alpha exp(\Delta F) \tag{22}$$

where $\Delta F = \ln(1-\phi_p) + \phi_p + \chi\phi_p{}^2 + \upsilon_{pw}^{\sim}\left(\phi_p{}^{\frac{1}{3}} - \phi_p{}^{\frac{5}{3}}\right)$, $\phi_p = \frac{\upsilon_{pw}^{\sim}}{(\alpha+\theta)+\upsilon_{pw}^{\sim}}$

α: Water adsorbed, nonbonded

θ: Water adsorbed, bonded

σ: Adsorption capacity parameter

ε: Molecular potential energy parameter

χ: Flory-Huggins parameter

$\upsilon_{pw}^{\sim}$: Specific volume ratio of biopolymer to water

The algorithm for fitting the parameters of the VCSM model is given below [49]:

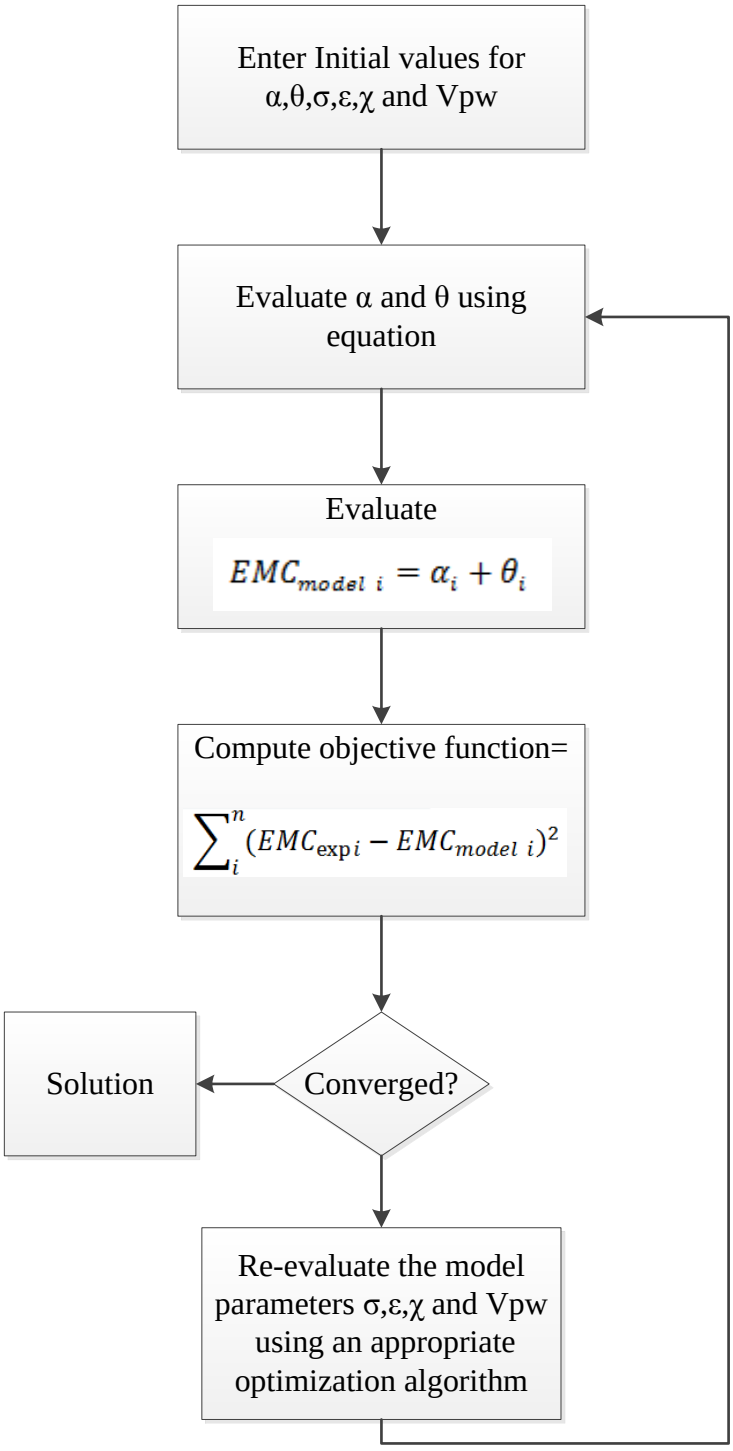

Figure 36. Algorithm for fitting the parameters of the VCSM model.

By applying the above algorithm, the behavior predicted by the VSCM model and the experiment data for eucalyptus are shown in Figure 37. Table 13 provides corresponding VSCM model parameters.

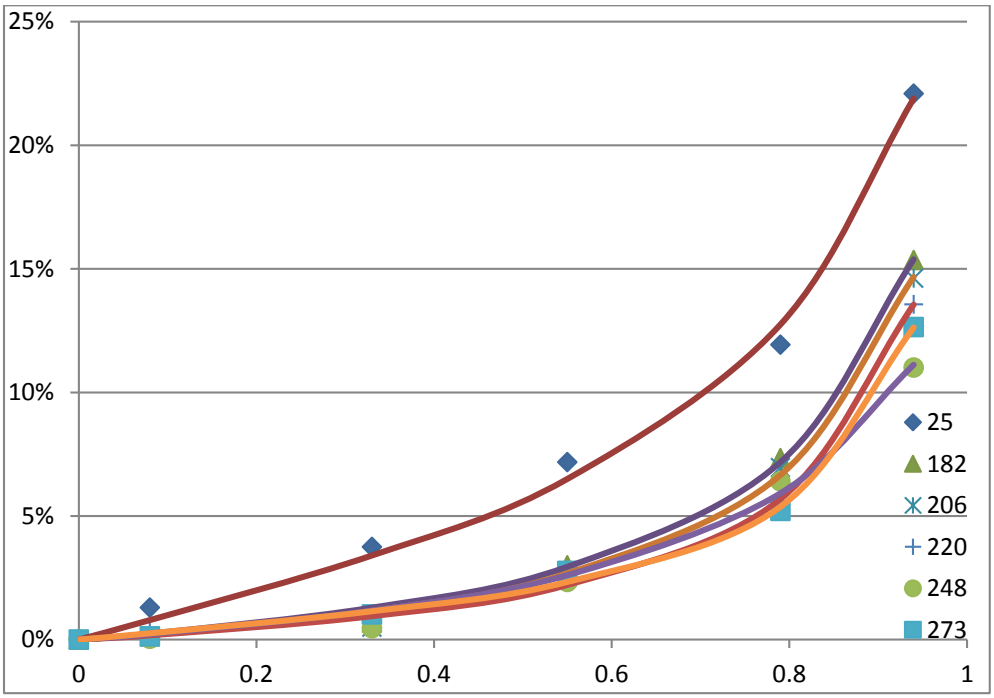

Figure 37. VSCM model of untorrefied and torrefied eucalyptus.

Table 13 – VSCM model parameters for figure 37.

	VSCM model parameters					
Torr. Temp. °C	α	θ	σ	ε	χ	Vpw
25	0.060	0.060	0.100	0.000	1.963	1.392
182	0.100	0.100	0.542	2.958	2.333	4.949
206	0.418	0.418	1.000	3.687	0.068	2.676
220	0.098	0.098	0.533	3.267	2.311	4.923
248	0.058	0.058	0.032	0.000	1.901	1.515
273	0.438	0.438	1.000	3.650	0.068	2.450

5.4 Electron microscopy

Scanning electron microscopy photos (SEM) obtained at the University of Hawaii Biological Electron Microscope Facility are shown in Figure 38. Leucaena and purple banagrass (S0) were tested to elucidate differences in surface structure and particle morphology between pre- and post- torrefied materials. All samples were subjected to the same amount of grinding. Figure 38 shows raw biomass samples have a relatively smooth surface, while the torrefied samples exhibit more cracks and fissures. This suggests biomass loses its bound fibrous structure and become brittle as a result of torrefaction. The reduced resistance to comminution can be explained by the thermochemical processes that occur during torrefaction. At a torrefaction temperature of 273°C, hemicellulose, lignin and cellulose, the main components of biomass cell walls, undergo depolymerization and recondensation, limited devolatilization and carbonization, and even carbonization (only hemicellulose) as shown in Figure 2. Depolymerization of cellulose decreases the length of the fibers and the breakdown of hemicellulose matrix, which bonds the cellulose fibers in biomass, causes loss of the tenacious nature of the biomass [7].

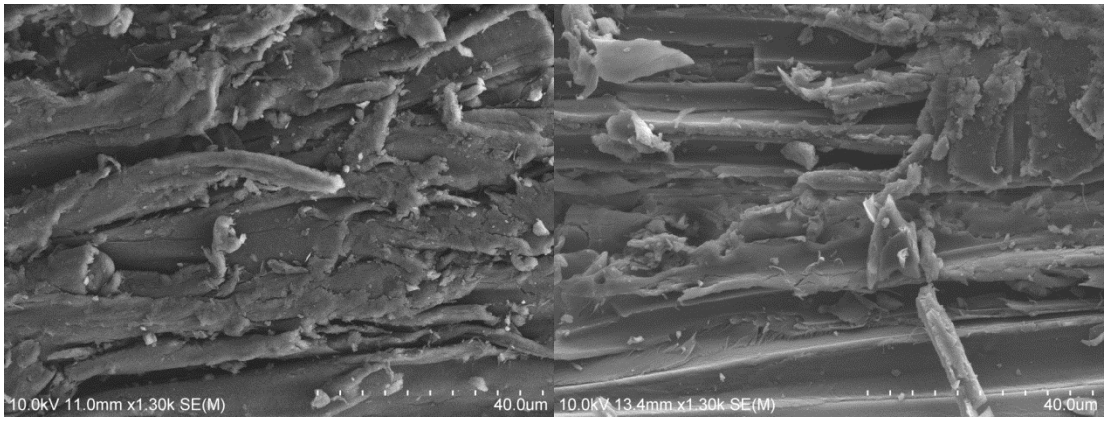

Raw leucaena Torrefied leucaena ($T_{torrefaction}$= 273°C)

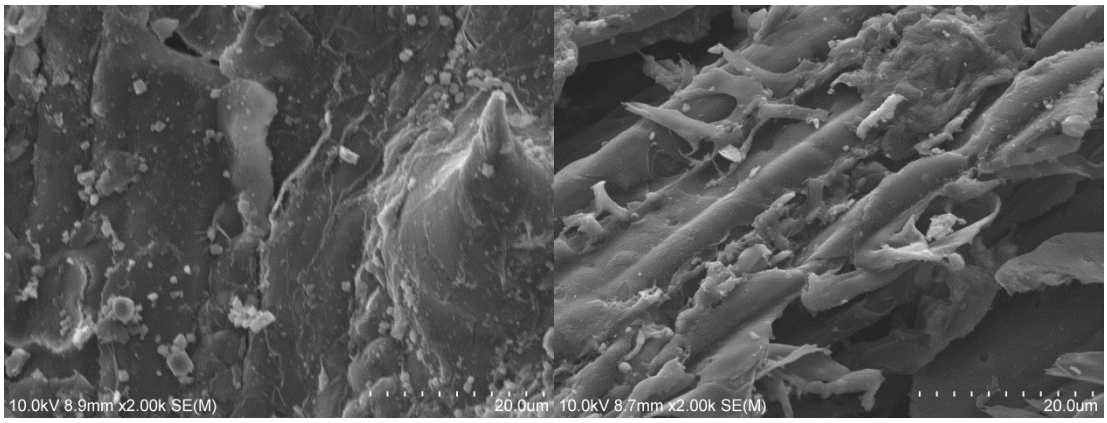

Raw P-Bana S0 Torrefied P-Bana S0 ($T_{torrefaction}$= 273°C)

Figure 38. SEM images of raw and torrefied leucaena and purple banagrass S0 after ball milling for 2 minutes at 165 rpm.

5.5 Economic evaluation

This section provides a general economic analysis of four alternative fuel processing scenarios. A spreadsheet was developed to perform the economic evaluation of the four scenarios to provide a relative cost comparison.

Table 14 – Four fuel processing scenarios to introduce biomass at a coal fired power plant. summarizes the four scenarios considered in the economic analysis. In **Scenario 1,** chipped and air dried biomass goes through dewatering/ leaching treatment and is then torrefied. The torrefied output is processed with the existing coal grinding equipment and feeding system in a coal fired power plant. Similarly, **Scenario 2** includes torrefaction equipment, and uses the existing coal grinding equipment and feeding system in the coal fired power plant; however, the chipped and air dried biomass samples are torrefied directly without dewatering/ leaching treatment. **Scenario 3** includes dewatering/ leaching treatment, biomass grinding equipment, and a biomass feed system installed in the coal fired power plant. **Scenario 4** includes biomass grinding equipment and a biomass feeding system in the coal fired power plant. In **Scenarios 3** and **4**, the biomass grinding equipment and biomass feeding system are installed in parallel with the existing coal preparation and feed system at the coal fired power plant.

Table 14 – Four fuel processing scenarios to introduce biomass at a coal fired power plant.

	Scenario			
	1	2	3	4
Primary biomass chipper	X	X	X	X
Dewatering/leaching treatment[1]	X		X	
Biomass dryer			X	X
Torrefaction system	X	X		
Coal grinding system	X	X		
Coal feeding system	X	X		
Biomass grinding system			X	X
Biomass feeding system			X	X
[1] Needed only for grass fuels, unnecessary for woody biomass				

The total processing cost includes capital costs and operating and maintenance (O&M) costs. The direct capital costs include plant construction, equipment costs, and installation but exclude engineering management costs. O&M costs include expenditures for energy, labor, management, and maintenance [68].

Cost data are summarized below and the spreadsheet for economic evaluation is shown in Table 15.

Table 15 – Economical evaluation spreadsheet of four alternative fuel processing scenarios.

	Capital cost $x1000	Capital cost $/Mg	Maintenance, tax, insurance, and other costs $/Mg	Energy Use kWh/Mg	Electricity cost[4] $/Mg	Total $/Mg	Mass Loss	M_p[5]/Mg	Scenario			
									1	2	3	4
Primary biomass chipper[1]						/	0%		X	X	X	X
Dewatering/leaching treatment[2]	407	0.20	0.16	12.35	3.30	3.79	5%	1.05 or 1.17	X		X	
Biomass dryer	4,500	2.16	1.80	45.00	12.02	15.98	0%	1.00			X	X
Torrefaction system[3]						66.2	10% or 20%	1.11 or 1.25	X	X		
Coal grinding system	0	0	0.80	36.00	9.62	10.42	0%	1.00	X	X		
Coal feeding system	0	0	0.04	67.20	17.95	17.99	0%	1.00	X	X		
Biomass grinding system	2,000	0.96	0.80	237.00	63.30	65.06	0%	1.00			X	X
Biomass feeding system	110	0.05	0.04	67.20	17.95	18.05	0%	1.00			X	X
Total Cost									106	111	103	99

[1] Needed for all four scenarios, cost not included for total cost comparison.

[2] Needed only for grass fuels, unnecessary for woody biomass, include $0.13/Mg leaching water cost.

[3] Total cost cited from Batidzirai et al. [69].
[4]Electricity cost is calculated based on an electricity rate of $0.2671/kWh.
[5]M_p is amount of feedstock processed to provide 1 Mg final product.

Electricity price – An electricity price of $0.2671/kWh was based on and average published rate for 2013 by Hawaiian Electric Company on the island of Oahu, for "Large Power Use Business, Directly Served." [Electricity rate retrieved from http://www.heco.com/heco/Residential/Electric-Rates/Average-Electricity-Prices-for-Hawaiian-Electric,-Hawaii-Electric-Light,-and-Maui-Electric, June 25, 2015]

Dewatering/leaching treatment – Turn et al. [70] studied process costs of dewatering/leaching treatment on banagrass. The total incremental cost for this operation was calculated to be $3.79/Mg.

Torrefaction system – A torrefication plant with input capacity of 250Gg of green wood per year (50% moisture content, wet basis) was used in this evaluation. Techno-economic evaluation of torrefaction of biomass materials was reported by Uslu et al. [71]. The total process cost of torrefied biomass was stated as €58 per Mg. Average exchange rate on 2008 is $1.47/€, which is $85.3 per Mg. Batidzirai et al. [69] gave the process costs as $66.2 per Mg. Tiffany et al. [72] stated the process cost is $42 per Mg for a torrefaction plant with capacity of 150 Gg per year. The lower unit cost reported by Tiffany for a smaller plant size does not obey common expectations associated with economies of scale. Cost data from Batidzirai et al. was used as the basis for the analysis in the present study.

Grinding system – Phanphanich and Mani measured specific grinding energy consumption of 237kWh/Mg for untorrefied biomass [11] and cite energy requirements for grinding coal of 7–36kWh/Mg. For this study, grinding energy for torrefied biomass is assumed to be 36kWh/Mg. The electricity rate for large commercial customers on Oahu is $0.2671 per kWh. Energy cost for biomass grinding would be $63.30/Mg. Similarly, coal and torrefied biomass grinding energy costs would be $9.62/Mg. The capital cost of a hammer mill for biomass fuel (250,000 Mg/yr) is

assumed to be $2.0 million USD in 2012 [73]. Assuming a fixed annual charge for capital of 12%, the capital cost of the hammer mill will be $0.96/Mg. Assuming annual maintenance, tax, insurance, and other costs of 10% of capital cost results in an additional cost of $0.80/Mg. Adding these costs to the electricity cost yields a total of $65.06/Mg of untorrefied biomass, while the torrefied biomass would use the existing the coal grinding system at a much lower cost, of $10.42/Mg.

Feeding system – Capital cost for feeding system is mainly the cost of the conveyor and hopper, which are estimated to be in a range from $30,000 to $70,000, each [70], [74]. A combined price for the two items of $110,000 was used in this evaluation. For a torrefaction system at scale of 250 Gg/yr., a capital cost of $0.05/Mg is calculated. Power requirement for the conveyor is estimated as 67.2kWh/Mg, the electricity cost is $17.95/Mg, and assumes annual maintenance, tax, insurance, and other costs equal to 10% of capital cost, which is $0.04/Mg. The total cost for a biomass feeding system is $18.05/Mg, compared to a total cost of $17.99/Mg for a coal feeding system.

Noticeable mass loss occurs in several steps of the four scenarios. An average mass loss of 5% is measured during the dewatering/leaching process. Mass loss during torrefaction is related to process conditions. Using AES coal as a benchmark and referring to Table 8 in section 5.1.1 and Table 11 in section 5.2, the mass loss and HHV associated with conditions required to produce torrefied biomass with an HGI values of 40 are listed in Table 16 for each of the fuels characterized earlier.

Table 16 – Summary of mass loss and higher heating values of each test fuel at conditions that produce an HGI equal to 40.

	Torr.Temp. for HGI≥40 [°C]	Mass Loss [%]	HHV [MJ/kg]
Leucaena	248	14.5	20.8
Eucalyptus	220	7.9	19.5
Energy Cane S0	206	16.9	19.3
Energy Cane S3	220	9.4	19.5
Purple Bana S0	220	16.2	18.6
Purple Bana S3	220	10.3	18.9
Sugar Cane S0	220	25.7	21.5
Sugar Cane S3	220	10.1	19.8
Sugar Cane Bagasse	220	9.7	18.6
S0 Average	215	19.6	19.8
S3 Average	220	9.9	19.4

As discussed in Section 5.1.1, dewatering/leaching treatment for grass fuels reduces the mass loss during torrefaction. A mass loss of 20% for S0 grass fuels and 10% for S3 were used in this evaluation.

A flow chart of four scenarios is shown below:

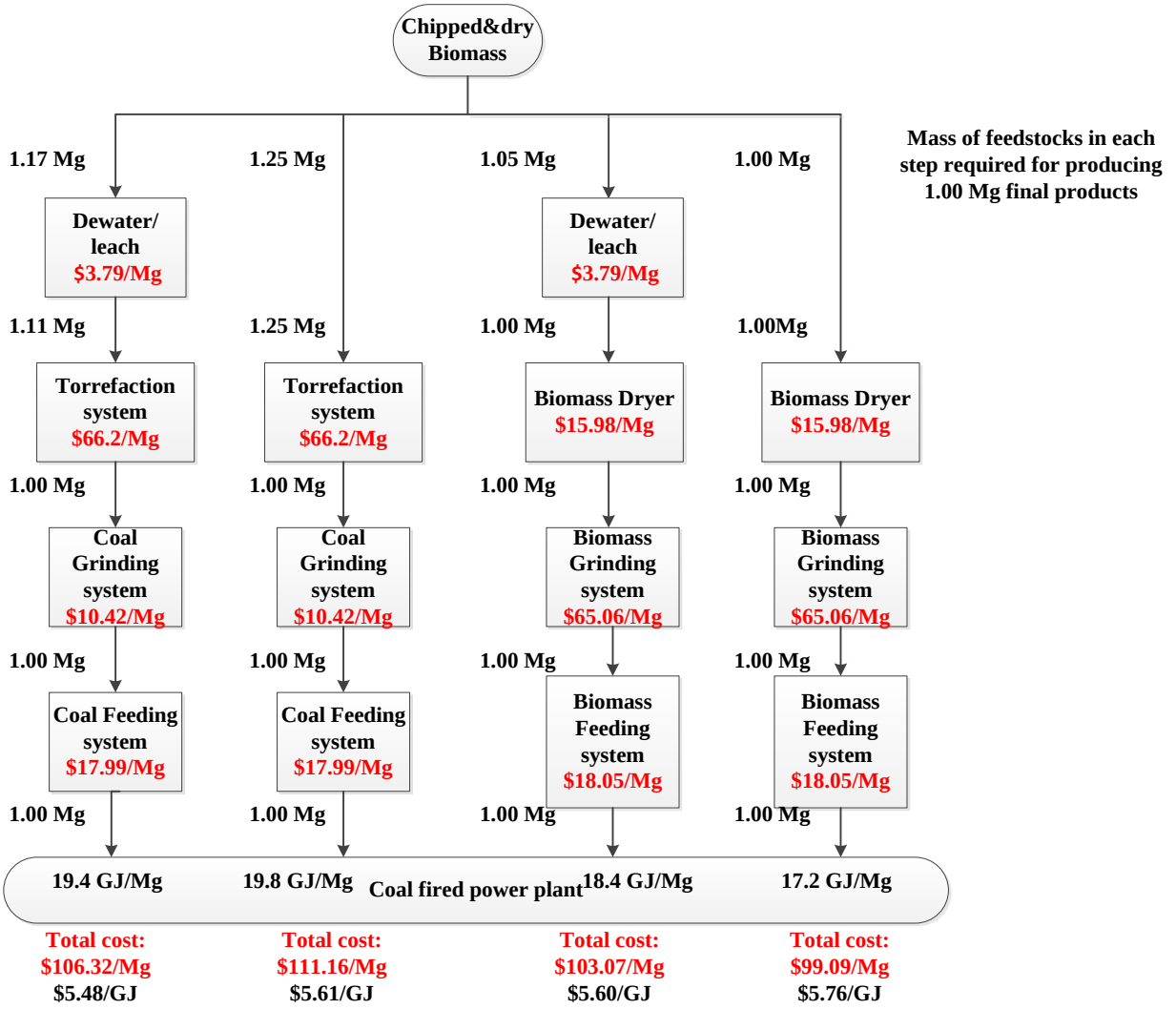

Figure 39. Fuel processing cost flow chart for four scenarios.

A sensitivity analysis was performed to identify the influence of electricity rate on fuel processing costs. The base value of electricity rate is $0.2671 per kWh, and this value was varied from -80% ($0.05 per kWh) to +80% ($0.48 per kWh). Figure 40 shows the fuel process costs increasing with electricity cost and all four scenarios reaching a common total cost of $5.52/GJ when electricity price is at a value of $0.26 per kWh. At electricity costs below the base case price of $0.26 per kWh, the fuel processing costs decrease more rapidly for scenarios 3 and 4

compared to scenarios 1 and 2. The analysis based on currently available data, indicates that the torrefaction process becomes cost effective at higher electricity rates.

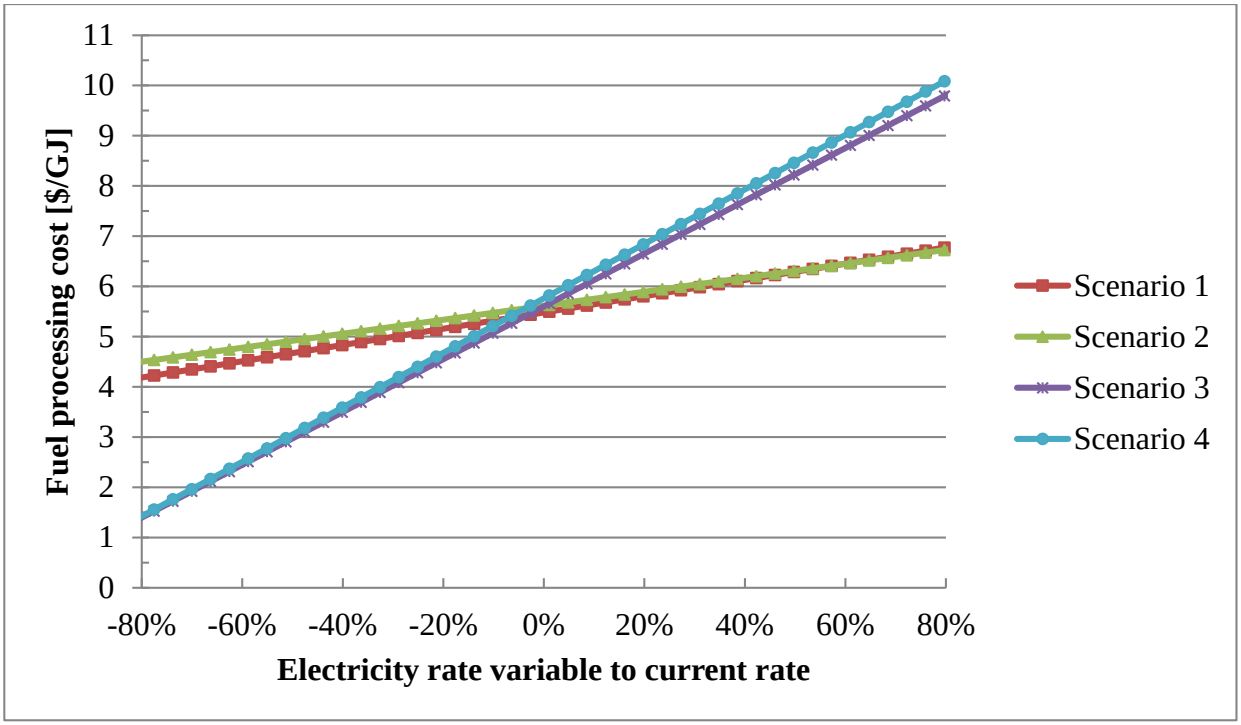

Figure 40. Fuel processing cost sensitivity to electricity costs relative to a base case cost of $0.2671 per kWh for four scenarios summarized in Table 14.

A sensitivity analysis was also performed to identify the influence of torrefaction cost on fuel processing costs.Figure 41 shows scenario 3 and 4 have constant fuel processing costs of $5.60/GJ and $5.76/GJ, respectively, because they do not include a torrefaction process. For scenarios 1 and 2, the fuel processing costs increase with increasing torrefaction costs and all four scenarios reaching a common processing cost of $5.67/GJ when torrefaction process cost is at $68/Mg. This value is near Batidziraiet al.'s estimated torrefaction cost of $66.20/Mg. At torrefaction processing costs below the base case price of $66.20/Mg, e.g. Tiffany et al.'s value of $57.1/Mg, the fuel processing costs are lower for scenarios 1 and 2 compared to scenarios 3

and 4. Above the base case price, the fuel processing costs increases more rapidly for scenarios 2 compared to scenarios 1, the result of higher mass loss when leaching and dewatering is employed. This economic analysis, using currently available cost data, indicates that including torrefaction as part of a fuel process is cost effective when the torrefaction processing cost is below $68/Mg.

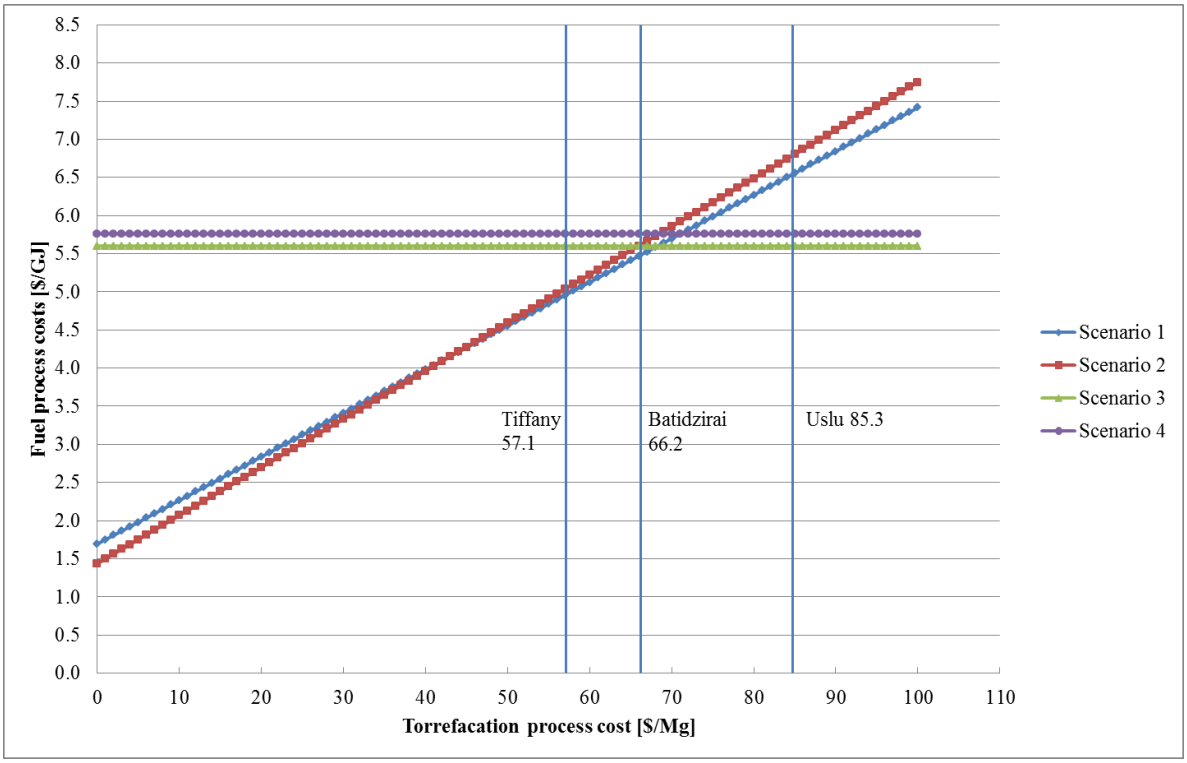

Figure 41. Fuel processing cost sensitivity to torrefaction process costs for four scenarios summarized in Table 14.

This economic analysis indicates that, at the current electricity rate of $0.2671 per kWh and torrefaction cost of $66.20/Mg, the fuel processing cost of the four scenarios are nearly equal, which are around $5.6/GJ. However, with an increased electricity rate and a lower torrefaction cost, scenarios with torrefaction included will become compelling. Furthermore, this economic analysis focuses on biomass processing. If the cost of biomass transportation and storage are

considered, then for torrefied biomass, the increase in energy density and improvement of biomass hydrophobicity would decrease transportation cost and storage cost. As a consequence, fuel process scenarios with torrefaction will become even more cost effective.

Cost of production data for sugarcane, banagrass, eucalyptus and leucaena were obtained from Tran et al.'s research [72]. The prices of sugarcane, banagrass, eucalyptus, and leucaena were $43.2/Mg, $65.0/Mg, $111.8/Mg and $59.5/Mg, respectively. Data of initial mass of feedstocks, HHVs of processed products and processing costs were cited from Figure 39 for each scenario. Feedstock cost and total cost of both feedstock and fuel processing were calculated for sugarcane, banagrass, eucalyptus and leucaena. Data are listed in Table **17**. The price of central Appalachia coal, as of 18-Sep-2015, was $53.6/Mg. With the assumption that HHV of coal is 30 GJ/Mg, according to Table 15, fuel processing of coal requires $10.42/Mg for coal grinding system and $17.99/Mg for coal feeding system at the current electricity rate, the total cost of both feedstock and fuel processing would be $2.73/GJ for coal. Under the assumptions used in this analysis the cost ($/GJ) of processed biomass fuels are roughly 3 to 4.7 times higher than that of processed coal.

Table 17 – Feedstock costs and total costs for sugarcane, banagrass, eucalyptus and leucaena under four scenarios summarized in Table 14.

		Scenario 1	Scenario 2	Scenario 3	Scenario 4
	Input mass [Mg]	1.2	1.3	1.1	1.0
	product HHV [MJ/kg]	19.4	19.8	18.4	17.2
	processing cost [$/GJ]	5.5	5.6	5.6	5.8
Sugarcane	Feedstock price [$/Mg]	43.2	43.2	43.2	43.2
	feedstock cost [$/GJ]	2.6	2.7	2.5	2.5
	total cost [2] [$/GJ]	8.1	8.3	8.1	8.3
Banagrass	Feedstock price [$/Mg]	65.0	65.0	65.0	65.0
	feedstock cost [$/GJ]	3.9	4.1	3.7	3.8
	total cost [2] [$/GJ]	9.4	9.7	9.3	9.5
Eucalyptus [1]	Feedstock price [$/Mg]		111.8		113.8
	feedstock cost [$/GJ]		7.1		6.6
	total cost [2] [$/GJ]		12.7		12.4
Leucaena [1]	Feedstock price [$/Mg]		59.5		61.5
	feedstock cost [$/GJ]		3.8		3.6
	total cost [2] [$/GJ]		9.4		9.3

[1] Dewater/leach treatment doesn't apply to eucalyptus or leucaena.

[2] Total cost is the summation of feedstock cost and processing cost.

6. Conclusion

All tested biomass species generally experienced increased mass loss and improved HHV with rising torrefaction temperature. HHVs of woody biomass were in the range of 19 – 22 MJ/kg. HHVs of grassy species, S0 and S3, were in the range of 17 – 26 MJ/kg and 18 – 23 MJ/kg, respectively.

All nine species of biomass had energy yields >95% at 182°C. When torrefaction temperature increased above 206 °C, the energy yields decreased at an increased rate. At comparable torrefaction temperatures below 248 °C, energy yields for woody and dewatered/leached (S3) grass species were substantially higher than unwashed (S0) grass species.

Proximate analysis verified that increasing torrefaction temperature resulted in increased fixed carbon content and decreased volatile matter content, and that the product became more energy dense. A Van Krevelen diagram constructed from ultimate analysis data showed that torrefaction of biomass follows a dehydration reaction pathway. Sugar cane S0 was determined to have the largest decrease in O/C and H/C value among all tested species.

All biomass samples had HGI values ~20 before torrefaction. Grindability of all samples improved noticeably with increased torrefaction level. Analysis of torrefied biomass showed that as torrefaction temperature increased, the particle size distribution approached curves generated for coal samples. Torrefaction temperatures ≤206°C produced modest increases in HGI. A transition was observed as torrefaction temperature increased from 206 to 220°C, producing increases in HGI value of ≥30% (relative). Using coal (HGI of 40) from the AES Hawaii Power Plant as a benchmark, torrefaction temperatures of 200 to 225 °C are recommended to attain

comparable grinding behavior in the torrefied biomass products. Leucaena is the exception requiring a torrefaction temperature of 260 °C.

In general, torrefaction improved hydrophobicity of all samples and hydrophobicity improved with increasing torrefaction temperature. Woody and dewatered/leached grass species (untorrefied and torrefied) were more hydrophobic than grass species that were not dewatered/leached (untorrefied and torrefied). S0 grass species (not dewatered/leached and untorrefied) exhibited the least degree of hydrophobicity.

Economic evaluation estimated a processing cost of $5.6/GJ for all biomass scenarios at the current electricity rate of $0.2671 per kWh and a torrefaction cost of $66.20/Mg. Sensitivity analyses indicated that with increased electricity rates and lower torrefaction costs, biomass processing scenarios that included torrefaction will become more cost effective than scenarios without torrefaction.

7. Recommendations for further studies

Torrefaction at 182, 206, 220, 248 and 273°C, with 30 min residence time has been investigated and results suggest that changes arising in fuel properties become more pronounced with increasing temperature. In future studies, extending the upper temperature limit to 300°C would be interesting. Variable residence times should also be explored.

Hardgrove Grindability Index has been used in this research. Another analytical method for measuring grindability could be by measuring energy usage of grinding different samples to certain fineness.

Hydrophobic characteristics of untorrefied and torrefied biomass have been studied. The impact of torrefaction on microbial durability would also be interesting to explore.

References

[1] US. Energy Information Administration, “Annual Energy Review 2011”. Washington: Office of Energy Statistics, U.S. Department of Energy, 2012.

[2] US Energy Information Administration, “Annual Energy Outlook 2012”. Washington: Office of Energy Statistics, U.S. Department of Energy, 2012.

[3] J. J. Chew and V. Doshi, “Recent advances in biomass pretreatment – Torrefaction fundamentals and technology,” Renewable and Sustainable Energy Reviews, vol. 15, no. 8, pp. 4212–4222, 2011.

[4] Honolulu: State of Hawaii, Department of Business, Economic Development and Tourism, “State of Hawaii Energy Resources Coordinator annual report,” pp. 2–4.

[5] Hawaiian Electric Company, “Clean Energy Update,” February, 2012.

[6] V. I. Keffer, S. Q. Turn, C. M. Kinoshita, and D. E. Evans, “Ethanol technical potential in Hawaii based on sugarcane, banagrass, Eucalyptus, and Leucaena,” Biomass and Bioenergy, vol. 33, no. 2, pp. 247–254, Feb. 2009.

[7] P. C. A. Bergman, “Torrefaction for entrained-flow gasification of biomass,” Energy research Centre of the Netherlands (ECN), 2005.

[8] D. Agar and M. Wihersaari, “Bio-coal, torrefied lignocellulosic resources – Key properties for its use in co-firing with fossil coal – Their status,” Biomass and Bioenergy, vol. 44, pp. 107–111, Sep. 2012.

[9] Y. Uemura, W. N. Omar, N. A. B. Othman, S. B. Yusup and T. Tsutsui, “Effect of atmosphere on torrefaction of oil palm wastes,” Bioengery Technology, 2011.

[10] G. Wang, Y. Luo, J. Deng, J. Kuang, and Y. Zhang, “Pretreatment of biomass by torrefaction,” Chinese Science Bulletin, vol. 56, no. 14, pp. 1442–1448, 2011.

[11] M. Phanphanich and S. Mani, “Impact of torrefaction on the grindability and fuel characteristics of forest biomass,” Bioresource Technology, vol. 102, no. 2, pp. 1246–1253, 2011.

[12] W. H. Chen and P. C. Kuo, “A study on torrefaction of various biomass materials and its impact on lignocellulosic structure simulated by a thermogravimetry,” Energy, vol. 35, no. 6, pp. 2580–2586, Jun. 2010.

[13] D. T. Ferro, “Torrefaction of agricultural and forest residues,” II-0185-FA conference publication, 2004.

[14] M. J. Prins, “Thermodynamic analysis of biomass gasification and torrefaction,” Ph.D. thesis, Eindhoven Technical University, The Netherlands, 2005.

[15] W. Yan, J. T. Hastings, T. C. Acharjee, C. J. Coronella& V. R. Vásquez, “Thermal Pretreatment of Lignocellulosic Biomass,” TCBiomass, 2009.

[16] M. J. C. van der Stelt, H. Gerhauser, J. H. A. Kiel, and K. J. Ptasinski, “Biomass upgrading by torrefaction for the production of biofuels: A review,” Biomass and Bioenergy, 2011.

[17] T. C. Acharjee, C. J. Coronella, and V. R. Vasquez, “Effect of thermal pretreatment on equilibrium moisture content of lignocellulosic biomass,” Bioresource technology, vol. 102, no. 7, pp. 4849–54, Apr. 2011.

[18] J. R. Arcate, “A new process for Torrefied wood manufacturing,” Bioenergy Update., vol. 2, no. 4, 2000.

[19] P. C. A. Bergman, “Torrefaction for biomass upgrading,” 14th European Biomass Conference & Exhibition, 2005.

[20] P. C. A Bergman, A. R. Boersma, R. W. R Zwart, and J. H. A Kiel, “Torrefaction for biomass co-firing in existing coal-fired power stations ‘biocoal,’” Energy research Centre of the Netherlands (ECN), 2005.

[21] J. P. Bourgeois and J. Doat, “Torrefied Wood from Temperate and Tropical Species. Advantages and prospects,” in Proceedings of Bioenergy 84, 1984, vol. 3, pp. 153–159.

[22] R. Pentananunt, A. N. M. M. Rahman, and S. C. Bhattacharya, “Upgrading of biomass by means of torrefaction,” Energy, vol. 15, no. 12.pp. 1175–1179, 1990.

[23] V. Repellin, A. Govin, M. Rolland, and R. Guyonnet, “Modeling anhydrous weight loss of wood chips during torrefaction in a pilot kiln,” Biomass and Bioenergy, vol. 34, no. 5, pp. 602–609, May 2010.

[24] A. Ohliger, M. Förster, and R. Kneer, “Torrefaction of beechwood: A parametric study including heat of reaction and grindability,” Fuel, 2012.

[25] R. H. H. Ibrahim, L. I. Darvell, J. M. Jones, and A. Williams, “Physicochemical characterisation of torrefied biomass,” Journal of Analytical and Applied Pyrolysis, Oct. 2012.

[26] P. Rousset, L. Macedo, J. M. Commandré, and A. Moreira, “Biomass torrefaction under different oxygen concentrations and its effect on the composition of the solid by-product,” Journal of Analytical and Applied Pyrolysis, vol. 96, pp. 86–91, Jul. 2012.

[27] B. Arias, C. Pevida, J. Fermoso, M. G. Plaza, F. Rubiera, and J. J. Pis, “Influence of torrefaction on the grindability and reactivity of woody biomass,” Fuel Processing Technology, vol. 89, no. 2, pp. 169–175, 2008.

[28] J. Wannapeera, B. Fungtammasan, and N. Worasuwannarak, “Effects of temperature and holding time during torrefaction on the pyrolysis behaviors of woody biomass,” Journal of Analytical and Applied Pyrolysis, vol. 92, no. 1, pp. 99–105, Sep. 2011.

[29] D. T. V. Essendelft, X. Zhou, and B. S. J. Kang, “Grindability determination of torrefied biomass materials using the Hybrid Work Index,” Fuel, vol. 105, pp. 103–111, Mar. 2013.

[30] W. Yan, T. C. Acharjee, C. J. Coronella, and V. R. Va, “Thermal Pretreatment of Lignocellulosic Biomass,” Environmental Progress & Sustainable Energy, vol. 28, no. 3, pp. 435–440, 2009.

[31] A. Pimchuai, A. Dutta, and P. Basu, “Torrefaction of Agriculture Residue To Enhance Combustible Properties,” Energy & Fuels, vol. 24, no. 9, pp. 4638–4645, Sep. 2010.

[32] T. G. Bridgeman, J. M. Jones, A. Williams, and D. J. Waldron, “An investigation of the grindability of two torrefied energy crops,” Fuel, vol. 89, no. 12, pp. 3911–3918, 2010.

[33] M. J. Prins, K. J. Ptasinski, and F. J. J. G. Janssen, “More efficient biomass gasification via torrefaction,” Energy, vol. 31, no. 15, pp. 3458–3470, 2006.

[34] T. G. Bridgeman, J. M. Jones, I. Shield, and P. T. Williams, “Torrefaction of reed canary grass, wheat straw and willow to enhance solid fuel qualities and combustion properties,” Fuel, vol. 87, no. 6, pp. 844–856, 2008.

[35] F. F. Felfli, C. A. Luengo, J. A. Suárez, and P. A. Beatón, “Wood briquette torrefaction,” Energy for Sustainable Development, vol. 9, no. 3, pp. 19–22, Sep. 2005.

[36] M. Pach, R. Zanzi, and E. Björnbom, “Torrefied Biomass a Substitute for Wood and Charcoal,” 6th Asia-Pacific International Symposium on Combustion and Energy Utilization, May, 2002.

[37] J. Deng, G. Wang, J. Kuang, Y. Zhang, and Y. Luo, “Pretreatment of agricultural residues for co-gasification via torrefaction,” Journal of Analytical and Applied Pyrolysis, vol. 86, no. 2, pp. 331–337, Nov. 2009.

[38] L. Shang, J. Ahrenfeldt, J. K. Holm, A. R. Sanadi, S. Barsberg, T. Thomsen, W. Stelte, and U. B. Henriksen, “Changes of chemical and mechanical behavior of torrefied wheat straw,” Biomass and Bioenergy, vol. 40, pp. 63–70, May 2012.

[39] C. J. Donahue and E. A. Rais, “Proximate Analysis of Coal,” Journal of Chemical Education, vol. 86, no. 2, p. 222, Feb. 2009.

[40] ASTM Standard D409, 2009, "Test Method for Grindability of Coal by the Hardgrove-Machine Method," ASTM International, West Conshohocken, PA, 2003, DOI: 10.1520/D0409_D0409M-12, www.astm.org.

[41] J. S. Tumuluru, L. G. Tabil, Y. Song, K. L. Iroba, and V. Meda, “Grinding energy and physical properties of chopped and hammer-milled barley, wheat, oat, and canola straws,” Biomass and Bioenergy, pp. 1–10, Nov. 2013.

[42] V. Repellin, A. Govin, M. Rolland, and R. Guyonnet, “Energy requirement for fine grinding of torrefied wood,” Biomass and Bioenergy, vol. 34, no. 7, pp. 923–930, Jul. 2010.

[43] G. Gray, M.R. Corcoran, W.H. Gavalas, “Pyrolysis of a wood-derived material. Effects of moisture and ash content,” Industrial and Engineering Chemistry Process Design and Development, vol. 24, pp. 646–651, 1985.

[44] ASTM Standard E104 - 02, 2012, "Practice for Maintaining Constant Relative Humidity by Means of Aqueous Solutions," ASTM International, West Conshohocken, PA, 2003, DOI: 10.1520/E0104-02R12, www.astm.org.

[45] L. Greenspan, “Humidity fixed points of binary saturated aqueous solutions,” Journal of Research of the National Bureau of Standards - A. Physics and Chemistry vol. 81, no. 1, 1977.

[46] ASTM Standard E871-72, 2013, "Test Method for Moisture Analysis of Particulate Wood Fuels," ASTM International, West Conshohocken, PA, 2003, DOI: 10.1520/E0871, www.astm.org.

[47] C. V. Berg, and S. Bruin, “Water Activity and its Estimation in Food Systems: Theoretical Aspects,” Academic Press. New York, 1981.

[48] ASAE Standards D245.5, “Moisture Relationships of Plant-based Agricultural Products,” ASAE, pp. 512–528, 1999.

[49] S. R. Bellur, C. J. Coronella, and V. R. Va, “Analysis of Biosolids Equilibrium Moisture and Drying,” Environmental Progress & Sustainable Energy, vol. 28, no. 2, pp. 291–298, 2009.

[50] V. R. Vasquez and C. J. Coronella, “A Simple Model for Vapor-Moisture Equilibrium in Biomass Substrates,” AIChE Journal, vol. 55, no. 6, 2009.

[51] D. Petersen, R. Link, C. Carll, and T. Highley, “Decay of Wood and Wood-Based Products above Ground in Buildings,” Journal of Testing and Evaluation, vol. 27, no. 2, p. 150, 1999.

[52] S. F. Curling, C. a Clausen, and J. E. Winandy, “Experimental method to quantify progressive stages of decay of wood by basidiomycete fungi,” International Biodeterioration & Biodegradation, vol. 49, no. 1, pp. 13–19, Jan. 2002.

[53] P. Verma, J. Dyckmans, H. Militz, and C. Mai, “Determination of fungal activity in modified wood by means of micro-calorimetry and determination of total esterase activity,” Applied microbiology and biotechnology, vol. 80, no. 1, pp. 125–33, Aug. 2008.

[54] M. Hakkou, M. Pétrissans, P. Gérardin, and A. Zoulalian, “Investigations of the reasons for fungal durability of heat-treated beech wood,” Polymer Degradation and Stability, vol. 91, no. 2, pp. 393–397, Feb. 2006.

[55] J. J. Weiland, R. Guyonnet, and C. Vera, “Study of chemical modifications and fungi degradation of thermally modified wood using DRIFT spectroscopy,” Hol zals Roh - und Werkstoff, vol. 61, pp. 216–220, 2003.

[56] D. P. Kamdem, A. Pizzi, and A. Jermannaud, “Durability of heat-treated wood,” Hol zals Roh- und Werkst, vol. 60, no. 1, pp. 1–6, Feb. 2002.

[57] K. Candelier, S. Dumarçay, A. Pétrissans, L. Desharnais, P. Gérardin, and M. Pétrissans, “Comparison of chemical composition and decay durability of heat treated wood cured under different inert atmospheres: Nitrogen or vacuum,” Polymer Degradation and Stability, vol. 98, no. 2, pp. 677–681, Feb. 2013.

[58] Ž. Šušteršic, A. Mohareb, M. Chaouch, M. Pétrissans, M. Petrič, and P. Gérardin, “Prediction of the decay resistance of heat treated wood on the basis of its elemental composition,” Polymer Degradation and Stability, vol. 95, no. 1, pp. 94–97, Jan. 2010.

[59] ASTM Standard D2017-05, 2013, "Test Method of Accelerated Laboratory Test of Natural Decay Resistance of Woods (Withdrawn 2014)," ASTM International, West Conshohocken, PA, 2003, DOI: 10.1520/D2017-05, www.astm.org.

[60] ASTM Standard D3172-13, "Practice for Proximate Analysis of Coal and Coke," ASTM International, West Conshohocken, PA, 2003, DOI: 10.1520/D3172, www.astm.org.

[61] ASTM Standard E872-82, 2013, "Test Method for Volatile Matter in the Analysis of Particulate Wood Fuels," ASTM International, West Conshohocken, PA, 2003, DOI: 10.1520/E0872, www.astm.org.

[62] ASTM Standard D1102-84, 2013, "Test Method for Ash in Wood," ASTM International, West Conshohocken, PA, 2003, DOI: 10.1520/D1102, www.astm.org.

[63] F. Akinrinola and L. Darvell, “HGI reference samples,” Personal communication, 2013.

[64] S. Van Loo and J. Kopperjan, “.Handbook of Biomass Combustion and Co-firing,” Earthscan. London, UK, vol. 2, 2008.

[65] F. Xu, K. Linnebur, and D. Wang, “Torrefaction of Conservation Reserve Program biomass: A techno-economic evaluation,” Industrial Crops and Products, vol. 61, pp. 382–387, Nov. 2014.

[66] B. Batidzirai, A. P. R. Mignot, W. B. Schakel, H. M. Junginger, and A. P. C. Faaij, “Biomass torrefaction technology: Techno-economic status and future prospects,” Energy, vol. 62, pp. 196–214, 2013.

[67] S. Q. Turn, C. M. Kinoshita, D. M. Ishimura, and B. M. Jenkins, “Removal of Inorganic Constituents of Fresh Herbaceous Fuels: Processes and Costs," Proceedings of the Third Biomass Conference of the Americas Montreal, Quebec, Canada, August 24-29, 1997,” pp. 1–14, 1997.

[68] A. Uslu, A. P. C. Faaij, and P. C. A. Bergman, “Pre-treatment technologies, and their effect on international bioenergy supply chain logistics. Techno-economic evaluation of torrefaction, fast pyrolysis and pelletisation,” Energy, vol. 33, no. 8, pp. 1206–1223, 2008.

[69] N. K. Tiffany, Douglas G., Won Fy Lee, Vance Morey, “Economic analysis of biomass torrefaction plants integrated with corn ethanol plants and coal-fired power plants,” Advanced Energy Resources, vol. 1, no. 2, pp. 127–146, 2013.

[70] J. Koppejan, S. Shahab, S. Melin, and S. Madrali, “Status overview of torrefaction technologies,” Energy Information Administration, Bioenergy, December, 2012.

[71] P. C. Badger, “Processing cost analysis for biomass feedstocks”, Oak Ridge National Laboratory, U.S. Department of Energy. 2002.

[72] N. Tran, P. Illukpitiya, J. F. Yanagida, and R. Ogoshi, “Optimizing biofuel production: An economic analysis for selected biofuel feedstock production in Hawaii,” Biomass and Bioenergy, vol. 35, no. 5, pp. 1756–1764, May 2011.